Locally instructed CXCR4hi neutrophils trigger environment-driven allergic asthma through the release of neutrophil extracellular traps

Coraline Radermecker[1,2,3,9], **Catherine Sabatel**[1,3,9], **Céline Vanwinge**[4], **Cecilia Ruscitti**[2,3], **Pauline Maréchal**[2,3], **Fabienne Perin**[4], **Joey Schyns**[1,2,3], **Natacha Rocks**[4], **Marie Toussaint**[5,6], **Didier Cataldo**[4], **Sebastian L Johnston**[5,6,7], **Fabrice Bureau**[1,3,8,10], **Thomas Marichal**[1,2,3,8,10]

[1]Laboratory of Cellular and Molecular Immunology

[2]Laboratory of Immunophysiology

[3]Faculty of Veterinary Medicine, Liege University, Liege, Belgium

[4]Laboratory of Tumor and Development Biology, GIGA Institute, Liege University, Liege, Belgium

[5]Airway Disease Section, National Heart and Lung Institute (NHLI), Imperial College London, London, UK

[6]Medical Research Council (MRC) and Asthma UK Centre in Allergic Mechanisms of Asthma, London, UK

[7]Imperial College Healthcare NHS Trust, London, UK

[8]WELBIO, Walloon Excellence in Life Sciences and Biotechnology, Wallonia, Belgium

Abstract

Low exposure to microbial products, respiratory viral infections and air pollution is a major risk factor for allergic asthma, yet the mechanistic links between such conditions and host

Corresponding authors: Thomas Marichal, Laboratory of Immunophysiology, GIGA Institute, Liege University, Quartier Hôpital, B34 Avenue de l'Hôpital 11, 4000 Liege, Belgium, t.marichal@uliege.be; Fabrice Bureau, Laboratory of Cellular and Molecular Immunology, GIGA Institute, Liege University, Quartier Hôpital, B34 Avenue de l'Hôpital 11, 4000 Liege, Belgium, fabrice.bureau@uliege.be.
[9]These authors contributed equally to this work and are co-first authors.
[10]These authors contributed equally to this work and are co-last authors.

susceptibility to type 2 allergic disorders remain unclear. Through the use of single-cell RNA sequencing (scRNA-seq), we characterized lung neutrophils in mice exposed to a pro-allergic, low dose of lipopolysaccharides (LPS[lo]) or a protective, high dose of LPS (LPS[hi]) before exposure to house dust mite (HDM). Unlike exposure to LPS[hi], exposure to LPS[lo] instructed recruited neutrophils to upregulate the expression of the chemokine receptor CXCR4 and to release neutrophil extracellular traps (NETs). The LPS^{lo}-induced neutrophils and NETs potentiated the uptake of HDM by CD11b^{+}Ly-6C^{+} dendritic cells (DCs) and type 2 allergic airway inflammation in response to HDM. NETs derived from CXCR4^{hi} neutrophils were also needed to mediate allergic asthma triggered by infection with influenza virus or exposure to ozone. Our study indicates that apparently unrelated environmental risk factors can shape recruited lung neutrophils to promote the initiation of allergic asthma.

Exposure to naturally occurring aeroallergens such as HDM, pollens or animal dander can, in some predisposed individuals, lead to allergic sensitization and the development of allergic asthma, a major public-health problem with high socio-economic impacts[1,2]. While genome-wide studies have discovered genetic polymorphisms associated with allergic susceptibility[3], the worldwide increase in the prevalence of allergies over the last decades points towards a major contribution of the environment[4,5]. Epidemiological studies have identified environmental risk factors for allergic asthma, including respiratory viral infections[6], air pollutants[7] or urban lifestyles associated with decreased exposure to microbes or their products such as bacterial endotoxins (LPS)[8,9]. A better understanding of the mechanisms by which pro-allergic environmental conditions shape the lung immune system to initiate allergic airway responses is an unmet and urgent need which may open novel therapeutic avenues for allergic asthma.

Allergic airway inflammation, a cardinal feature of allergic asthma, is thought to result from an aberrant type 2 immune response directed against inhaled allergens[10,11]. The initiation of type 2 immunity to HDM, a major allergen source in humans[12], involves sensing of LPS and compounds of HDM by epithelial cells and the release of pro-allergic alarmins that instruct lung DCs to sample allergens, transport them to the draining lymph node (LN) and induce allergen-specific CD4^{+} T helper type 2 (T_H2) cells. Upon subsequent HDM challenge, T_H2 effector cells secrete type 2 cytokines such as IL-4, IL-5 and IL-13, which orchestrate features of allergic airway inflammation, including airway eosinophilia and goblet cell metaplasia through IL-5- and IL-13-dependent mechanisms, respectively[11,13].

Neutrophils are known to function as first-responders specialized in pathogen clearance and as prototypic effector cells of type 17 responses. However, new evidence points to the complexity and functional diversity of neutrophils[14,15]. The role of neutrophils in asthma has mainly been investigated in severe asthma, which is characterized by a type 17-mediated neutrophilic inflammation[16–19]. In type 2 allergic asthma, the role of neutrophils has been investigated in the effector phase, but not the initiation, of type 2 responses[17,20]. Indeed, neutrophil-derived DNA found in NETs, which also contain modified histone proteins such as citrullinated histone H3 (Cit-H3) and granule proteins such as neutrophil elastase (NE) and myeloperoxidase (MPO)[15], contributed to the manifestations of rhinovirus-induced allergic asthma exacerbations[20].

Here, using single-cell RNA-sequencing (scRNA-seq) and mouse models of allergic asthma triggered by three distinct pro-allergic environmental factors, we found that locally-programmed, NET-releasing CXCR4^{hi} lung neutrophils acted as early triggers of type 2 allergic airway inflammation. Our results indicate that phenotypically and functionally distinct tissue neutrophils act as common determinants of environment-driven allergic asthma onset in mice.

Results

Low-dose LPS exposure potentiates HDM-induced allergic asthma

To investigate the mechanisms of environment-driven initiation of allergic asthma in mice, we used a model of exposure to HDM in mice pre-exposed to a pro-allergic environmental factor, namely a low dose of LPS[21]. Different doses of LPS, ranging from 0.1ng to 10μg, were administered intranasally (i.n.) to groups of BALB/c mice, which were exposed 1 and 8 days later to 40 and 10 μg HDM i.n., respectively. At day 11, airway eosinophilia, a feature of type 2 allergic asthma[11], was virtually absent in vehicle pre-exposed HDM-treated mice, but reached a peak in mice pre-exposed to 100ng LPS, and returned to baseline with 10μg LPS (Supplementary Fig. 1a,b). Single exposures to either 100ng or 10μg LPS were chosen to model a pro-allergic, 'hygienic' (LPS[lo]) or a protective[22], 'non-hygienic' (LPS[hi]) environment, respectively. LPS[lo] mice treated with HDM (LPS[lo]-HDM mice) developed features of allergic asthma 3 days after the second HDM instillation, including increased bronchial hyperreactivity to methacholine (Fig. 1a), airway eosinophilia (Fig. 1b), a higher secretion of IL-4, IL-5 and IL-13 by total LN cells restimulated with HDM (Fig. 1c), perivascular and peribronchial leukocyte infiltration (Fig. 1d,e), and increased bronchial mucus production (Fig. 1f,g) when compared to vehicle-HDM or LPS^{hi}-HDM mice. Of note, CD45^{+}CD11b^{hi}Ly-6G^{hi} neutrophils, quantified by flow cytometry, were massively recruited into the lungs of LPS^{lo} and LPS^{hi} mice between 6 and 24 h after LPS exposure (Supplementary Fig. 1c,d). Thus, low-dose exposure to LPS induced a lung environment that promoted type 2 immunity to HDM and the development of allergic asthma.

scRNA-seq identifies particular neutrophils in LPS[lo] mice

To investigate the transcriptional diversity of lung neutrophils, we performed scRNA-seq. Twenty-four h after vehicle, LPS[lo] and LPS[hi] i.n., neutrophils were first enriched from lung single-cell suspensions pooled from 3 BALB/c mice per condition by negative selection using magnetic-activated cell sorting (MACS) and were then FACS-sorted as CD45^{+} cells (Supplementary Fig. 2a-c). Using the 10x Genomics platform[23], cells were subjected to single cell droplet encapsulation, scRNA-seq and quality control filtering (Supplementary Fig. 2d,e). A total of 1,406, 2,146 and 2,746 cells were analyzed in vehicle, LPS[lo] and LPS[hi] mice, respectively. Non-linear dimensional reduction and graph-based clustering of single cells pooled from vehicle, LPS[lo] and LPS[hi] mice identified 6 transcriptionally distinct clusters of neutrophils, all characterized by high expression of *S100a8*, *S100a9* and *Csf3r* transcripts (cluster 0 – cluster 5; Fig. 2a and Supplementary Fig. 2f,g). Neutrophils from vehicle lungs were grouped in one cluster (cluster 0; Fig. 2b-d and Supplementary Fig. 3a-d), while neutrophils from LPS[lo] and LPS[hi] mice were segregated into 5 additional clusters (clusters 1-5, Fig. 2b-d). Neutrophils in cluster 1 were almost uniquely found in lungs from

LPS[lo] mice, while neutrophils in clusters 2, 3 and 5 were nearly exclusively present in lungs from LPS[hi] mice and neutrophils in cluster 4 were equally distributed between LPS[hi] and LPS[lo] mice (Fig. 2b-d). We performed a differential expression analysis and we defined a common, dose-independent, LPS-induced signature as the list of transcripts that were commonly upregulated in each of the clusters 1 to 5 as compared to cluster 0 (Supplementary Fig. 3e,f). We then identified LPS[lo] or LPS[hi] signatures as the lists of transcripts that were upregulated in cluster 1 or clusters 2,3 and 5, respectively, as compared to cluster 0, and that were absent from the common LPS signature. *Cxcr4* and *Lamp-1* transcripts, which code for proteins detectable by flow cytometry, were significantly upregulated in LPS[lo] neutrophils as compared to LPS[hi] neutrophils (Fig. 2e). The LPS[hi] signature comprised 25 transcripts that were enriched in processes such as complement receptor-mediated signaling pathways (*Fpr1, Fpr2*) and response to type 1 or type 2 interferon (IFN) (*Ifitm1, Ifitm3, Ifi47*) based on Gene Ontology (GO) analysis (Fig. 2e-g). The LPS[lo] signature contained 97 transcripts that were enriched in genes involved in endoplasmic reticulum stress (*Atf3, Atf4, Bax*), reactive oxygen species synthesis (*Ptgs2, Arg2, Il1b*), oxidative stress (*Rps3, Prdx6, Jun*) and ERK1/2 signaling cascade (*Cd74, C3, Hmgb1*) (Fig. 2e,f,h), responses that have all been implicated in the formation and release of NETs[15,24]. Thus, lung neutrophils induced by a pro-allergic, low dose of LPS are transcriptionally distinct from those induced by a high LPS dose.

LPS[lo] locally triggers NET-releasing CXCR4^{hi} neutrophils

To validate the scRNA-seq findings and identify the neutrophils induced by LPS^{lo} treatment *in vivo*, we exposed BALB/c mice to vehicle, LPS^{lo} or LPS^{hi} treatment and assessed the expression of CXCR4 and Lamp-1 on lung CD45^{+}CD11b^{hi}Ly-6G^{hi} neutrophils 24 h later. We found a significant upregulation of CXCR4 and Lamp-1 on lung neutrophils from LPS^{lo} mice as compared to neutrophils from vehicle or LPS[hi] mice (Fig. 3a,b). The expression of CD49d, an integrin reported to be highly expressed on CXCR4^{hi} blood neutrophils[25], was also upregulated on lung neutrophils from LPS^{lo} mice (Fig. 3a,b). Next, we performed time-course analyses of CXCR4 expression on bone marrow (BM), blood and lung CD45^{+}CD11b^{hi}Ly-6G^{hi} neutrophils isolated 6, 12, 18, 24 and 48 h after treatment in vehicle, LPS^{lo} and LPS^{hi} mice. In the lung, CXCR4 expression on CD45^{+}CD11b^{hi}Ly-6G^{hi} neutrophils started to increase 18 h after LPS^{lo}, reached a peak at 24 h and returned to baseline after 48 h (Fig. 3c). Expression of CXCR4 on lung CD45^{+}CD11b^{hi}Ly-6G^{hi} neutrophils from LPS^{hi} mice was similar to that of vehicle mice (Fig. 3c). Of note, while we detected a rhythmic oscillation in the expression of CXCR4 expression on blood neutrophils[26], the oscillation was not affected by treatment with LPS, regardless of the dose (Fig. 3c). Expression of CXCR4 on BM CD45^{+}CD11b^{hi}Ly-6G^{hi} neutrophils was similar in LPS^{lo} and vehicle mice (Fig. 3c), indicating that low-dose LPS administered i.n. instructs the neutrophils locally, and not at distant sites. Morphologically, CXCR4^{hi}CD49d^{hi} neutrophils sorted from lungs of LPS^{lo} mice were smaller and displayed a higher nucleus/ cytoplasm ratio and a hypersegmented nucleus compared to lung CXCR4^{lo}CD49d^{lo} neutrophils from LPS^{hi} mice (Fig. 3d and Supplementary Fig. 4a-d).

Lung CXCR4^{hi}CD49d^{hi} neutrophils sorted from LPS^{lo} mice released NETs *ex vivo*, while lung CXCR4^{lo}CD49d^{lo} neutrophils from vehicle or LPS^{hi} mice did not (Fig. 3e and

Supplementary Fig. 4e-g). In addition, the amount of free double-stranded DNA (dsDNA) and of NE/DNA complexes, which are characteristic of NETs[15], were higher in the broncho-alveolar lavage fluid (BALF) of LPS[lo] mice 24 h post-LPS as compared to vehicle and LPS[hi] mice (Fig. 3f,g), while the amounts of Cit-H3, a modified form of histone H3 implicated in chromatin decondensation and NET formation[15], were specifically increased in the lungs of LPS[lo] mice (Fig. 3h,i). High-resolution confocal microscopy indicated the presence of extracellular MPO[+]Cit-H3[+] NETs in the lungs of LPS[lo] mice, unlike in vehicle or LPS[hi] mice (Fig. 3j,k). Notably, neutrophil depletion with an antibody against Ly-6G was associated with an absence of NETs 24 h after LPS in the lungs of anti-Ly-6G-treated LPS[lo] mice (Supplementary Fig. 5), indicating that NETs were exclusively derived from neutrophils. Concordant with the upregulation of CXCR4, NETs were detected at 18 h after low-dose LPS, but not detected after 48 h (Supplementary Fig. 6a,b). These observations indicate that neutrophils recruited to the lungs of LPS^{lo} mice had a CXCR4^{hi}CD49d^{hi}Lamp-1^{hi} phenotype that was only detected in the lungs, and were prone to release NETs, while lung neutrophils recruited in LPS^{hi} mice were phenotypically similar to steady-state neutrophils and did not release NETs.

CXCR4[hi] neutrophils and NETs trigger allergic airway inflammation in LPS[lo] mice

To address whether the effect of low-dose LPS on HDM-induced allergic airway inflammation was mediated by neutrophils, LPS[lo]-HDM mice were administered Sch527123, an antagonist of the chemokine receptor CXCR2 (anti-CXCR2)[27], orally 2 h before and 4 and 8 h after LPS[lo], and 2 h before and 4 h after i.n. administration of 40 μg HDM in order to inhibit the LPS-induced neutrophil recruitment to the lung[28]. Treatment with anti-CXCR2 significantly reduced numbers of lung CD45^{+}CD11b^{hi}Ly-6G^{hi} neutrophils 24 h after LPS treatment in LPS^{lo} mice (Fig. 4a,b). LPS^{lo}-HDM mice treated with anti-CXCR2 had significantly reduced airway eosinophilia (Fig. 4c), HDM-specific type 2 immune responses (Fig. 4d), perivascular and peribronchial inflammation (Fig. 4e,f) and mucus cell production (Fig. 4g,h) compared to vehicle LPS^{lo}-HDM mice. In a different approach, we isolated lung neutrophils from vehicle, LPS^{lo} or LPS^{hi} mice by MACS negative selection and FACS CD45^{+} sorting 24 h post-LPS (vehicle, LPS^{lo} and LPS^{hi} neutrophils, respectively) and adoptively transferred 5×10^5 neutrophils in the trachea of naive recipients together with 40 μg HDM, which were exposed to 10 μg HDM i.n. 7 days later and analyzed 11 days after transfer. Transfer of LPS[lo] neutrophils was sufficient to trigger airway eosinophilia (Fig. 4i), HDM-specific type 2 immunity (Fig. 4j), peribronchial inflammation (Fig. 4k,l) and increased mucus production (Fig. 4m,n) in HDM-treated recipient mice, while all these features were significantly lower in mice that received vehicle or LPS[hi] neutrophils.

To test the contribution of NETs to the initiation of allergic airway inflammation in LPS[lo]-HDM mice, we targeted the NETs with 4 daily intraperitoneal (i.p.) injections of DNAse, which degrades NETs[20,29], starting one day before LPS[lo] treatment, or with 8 i.p. injections of either the neutrophil elastase inhibitor GW-311616 (NEi)[15] or an inhibitor of the arginine deiminase PAD4 (Cl-amidine)[30], every 12 h starting one day before LPS[lo] treatment. Treatments with DNAse, NEi and Cl-amidine resulted in a significant decrease of NET volume in LPS[lo] mice 24 h post-LPS (Fig. 5a,b). Most features of type 2 allergic airway

inflammation, such as airway eosinophilia (Fig. 5c), HDM-specific type 2 immunity (Fig. 5d), peribronchial inflammation (Fig. 5e,f) and increased mucus production (Fig. 5g,h) were significantly reduced in DNAse-, NEi - or Cl-amidine-treated LPS[lo]-HDM mice compared to vehicle LPS[lo]-HDM mice, except for LN production of IL-4 and IL-13, which was similar in DNAse- and NEi-treated LPS[lo]-HDM mice, respectively, compared to vehicle LPS[lo]-HDM mice (Fig. 5d), and mucus production in NEi-treated LPS[lo]-HDM mice compared to vehicle LPS[lo]-HDM mice (Fig. 5g,h). These observations indicate that lung neutrophils and NETs from LPS^{lo} mice were mediating the pro-allergic effects of low-dose LPS on HDM-induced allergic asthma.

NETs promote HDM uptake by CD11b^{+}Ly-6C^{+} DCs

Given the predominant role played by lung DCs in the induction of T_H2 responses to HDM[31,32], we looked at their ability to take up HDM upon exposure to vehicle, LPS^{lo} or LPS^{hi}. Twenty-four h post-LPS, we administered 40 μg fluorescent-labeled AF647-HDM i.n. and the numbers of lung CD45^{+}CD11c^{hi}MHC-II^{hi}HDM^{+} DCs were quantified 24 h later by flow cytometry. Lungs of LPS^{lo} mice exposed to AF647-HDM had greater numbers of CD11b^{+}Ly-6C^{+} DCs, and to a lesser extent CD11b^{+}Ly-6C^{-} DCs, that were AF647-HDM^{+} compared to lungs of vehicle or LPS^{hi} mice (Fig. 6a-c). Of note, the numbers of CD11b^{+}Ly-6C^{+}AF647-HDM^{+} DCs were significantly reduced in DNAse, NEi or Cl-amidine-treated LPS^{lo}-AF647-HDM mice as compared to vehicle LPS^{lo}-AF647-HDM mice (Fig. 6d), suggesting that NETs promoted HDM uptake by CD11b^{+}Ly-6C^{+} DCs directly or indirectly.

To assess whether LPS^{lo} neutrophils modulated AF647-HDM uptake by CD11b^{+}Ly-6C^{+} DCs directly, we co-cultured vehicle, LPS^{lo} or LPS^{hi} neutrophils with bone-marrow derived DCs (BMDCs), which contained both CD11b^{+}Ly-6C^{+} and CD11b^{+}Ly-6C^{-} BMDCs (Fig. 6e) and are known to induce type 2 sensitization to HDM when pulsed with HDM and reinjected into recipient animals[33]. Co-culture of AF647-HDM-treated BMDCs with LPS^{lo} neutrophils increased the uptake of AF647-HDM by CD11b^{+}Ly-6C^{+} BMDCs, and to a lesser extent by CD11b^{+}Ly-6C^{-} BMDCs as compared to AF647-HDM-treated BMDCs alone (Fig. 6f). Co-culture of AF647-HDM-treated BMDCs with vehicle or LPS^{hi} neutrophils promoted a marginal increase in AF647-HDM uptake by CD11b^{+}Ly-6C^{+} BMDCs compared to AF647-HDM-treated CD11b^{+}Ly-6C^{+} BMDCs alone, which was significantly lower than that elicited by the co-culture of AF647-HDM-treated BMDCs with LPS^{lo} neutrophils (Fig. 6f). AF647-HDM uptake, especially by CD11b^{+}Ly-6C^{+} BMDCs, was significantly diminished when DNAse was added to the co-culture of BMDCs with LPS^{lo} neutrophils (Fig. 6f), indicating that the process was dependent on NETs. Co-culture of BMDCs with LPS^{lo} neutrophils, but not with vehicle or LPS^{hi} neutrophils, promoted the expression of the pro-T_H2 co-stimulatory molecule CD86[34,35] on CD11b^{+}Ly-6C^{+} BMDCs, and this effect was not affected by DNAse treatment (Fig. 6f). Thus, LPS^{lo} neutrophils acted on CD11b^{+}Ly-6C^{+} DCs directly to promote AF647-HDM uptake through NET-dependent mechanisms.

Other pro-allergic factors promote allergic asthma via NETs

Next, we tested whether NET-prone CXCR4^{hi} neutrophils were associated with additional pro-allergic conditions. Besides low exposure to microbial products, respiratory viral

infections[6] and air pollution[7] also represent risk factors for allergic asthma in humans. In mice, acute respiratory infection with influenza virus[36] or exposure to ozone[37] promote allergic airway inflammation to HDM or ovalbumin, respectively. BALB/c mice infected i.n. with 5 plaque-forming units (PFU) of influenza A virus H1N1 strain PR8/34 (PR8) had decreased body weight at day 7 (Supplementary Fig. 7a,b), and increased lung viral RNA expression (Supplementary Fig. 7c) and numbers of $CD45^+CD11b^{hi}Ly-6G^{hi}$ neutrophils (Supplementary Fig. 7d) between 3 and 7 days after infection. Similarly, BALB/c mice exposed for 3 days to 2 ppm ozone during 3 h also had increased lung neutrophil numbers 24 h after the last exposure (Supplementary Fig. 7e,f). Seven days after PR8 or 24 h after ozone exposure, these neutrophils had increased expression of CXCR4, Lamp-1 and CD49d as compared to neutrophils from uninfected or air-exposed control mice (Fig. 7a-d), suggesting shared phenotypical similarities with LPS^{lo} neutrophils. In addition, $CXCR4^{hi}$ neutrophils were only found in the lung and could not be detected in the blood or BM (Fig. 7e,f), suggesting local imprinting. NETs were also found in the lungs of mice infected with PR8 or exposed to ozone (Fig. 7g-n and Supplementary Fig. 7g-k), suggesting exposure to other pro-allergic factors triggered the accumulation of NET-prone $CXCR4^{hi}$ neutrophils in the lungs.

Next, we instilled PR8-infected mice i.n. with 40 μg HDM 7 days after PR8 and with 10 μg HDM 7 days later (PR8-HDM). To test the contribution of NETs to PR8-triggered allergic asthma, PR8-HDM mice were treated daily for 12 days with DNAse i.p., starting 5 days after PR8. Alternatively, PR8-HDM mice were treated every 12 h with NEi or Cl-amidine i.p. for the same duration as for DNAse. Three days after the HDM challenge, we observed increased susceptibility of PR8-HDM mice to develop airway eosinophilia and HDM-specific IgG1 (Fig. 8a), HDM-specific type 2 immunity (Fig. 8b) and goblet cell hyperplasia (Fig. 8c,d), while administration of HDM without pre-exposure to PR8 did not induce features of allergic asthma, and treatments of PR8-HDM mice with DNAse, NEi and Cl-amidine resulted in a significant decrease of nearly all features of allergic asthma compared to vehicle PR8-HDM mice, except for LN production of IL-13, which was similar in DNAse-treated and vehicle PR8-HDM mice (Fig. 8b). In addition, while we observed higher numbers of lung $CD11b^+Ly-6C^+AF647-HDM^+$ DCs in PR8-AF647-HDM mice compared to uninfected AF647-HDM-treated controls 24 h after AF647-HDM, these numbers were significantly decreased in DNAse, NEi- and Cl-amidine-treated PR8-AF647-HDM mice compared to vehicle PR8-AF647-HDM controls (Fig. 8e).

We also instilled ozone-exposed mice i.n. with 40 μg HDM 1 day after the last ozone treatment and with 10 μg HDM 7 days later (ozone-HDM). Some ozone-HDM mice mice were also treated daily for 4 days with DNAse i.p., starting the first day of ozone exposure. Alternatively, ozone-HDM mice were treated every 12 h with NEi or Cl-amidine i.p. for the same duration as for DNAse. Three days after the HDM challenge, we observed increased susceptibility of ozone-HDM mice to develop airway eosinophilia and HDM-specific IgG1 (Fig. 8f), HDM-specific type 2 immunity (Fig. 8g), goblet cell hyperplasia (Fig. 8h,i) and peribronchial inflammation (Supplementary Fig. 8), while administration of HDM without pre-exposure to ozone did not induce features of allergic asthma, and treatments of ozone-HDM mice with DNAse, NEi and Cl-amidine resulted in a significant decrease of all the features of allergic asthma tested (Fig. 8f-i and Supplementary Fig. 8). In addition, while we

observed higher numbers of lung CD11b^{+}Ly-6C^{+}AF647-HDM^{+} DCs in ozone-AF647-HDM mice compared to air-exposed AF647-HDM-treated controls 24 h after AF647-HDM, these numbers were significantly decreased in DNAse, NEi- and Cl-amidine-treated ozone-AF647-HDM mice compared to vehicle ozone-AF647-HDM controls (Fig. 8j).

These observations suggested that NETs promoted AF647-HDM uptake by lung CD11b^{+}Ly-6C^{+} DCs and mediated allergic airway inflammation triggered by flu infection or ozone exposure.

Discussion

Here we showed that neutrophils have an important role in type 2 allergic immunity and link pro-allergic environmental conditions and host allergic susceptibility. We showed that airway exposure to low-dose LPS, influenza virus infection and ozone exposure in mice induced the accumulation of NET-releasing CXCR4^{hi} neutrophils in the lung. These neutrophils promoted the uptake of HDM by lung CD11b^{+}Ly-6C^{+} DCs and increased susceptibility to allergic asthma.

LPS measurements have been used in epidemiological studies related to the 'hygiene hypothesis', suggesting that an LPS-rich environment is associated with reduced risk of atopy and asthma, while LPS-poor environments represent a risk factor for the development of asthma[8,38]. The 'hygienic' model used here is an adaptation of a previous model[21], in which priming with a low or high dose of LPS biased the immune response to ovalbumin towards a T_H2 or T_H1 profile, respectively. Here, we found that exposure to a low dose of LPS in BALB/c mice potentiated HDM-induced type 2 allergic asthma, while priming with a higher dose of LPS[22] had no substantial effect.

Airway exposure to low-dose LPS in mice triggered NET-releasing CXCR4^{hi} neutrophils in the lung. These neutrophils shared similarities with 'aged' neutrophils, a subset of NET-prone CXCR4^{hi} neutrophils found in the blood[25,26]. Kinetic analyses of CXCR4 expression on lung, blood and BM neutrophils indicated that neutrophils were recruited to the lung and instructed locally. This indicates that CXCR4^{hi} neutrophils, rather than representing a subset, are in a transient state of activation that depends on a local stimulus (i.e., low-dose LPS). Our data argue in favor of the notion that neutrophils are heterogenous, plastic, and can adapt to context-specific cues to exert particular functions[14]. We found that these locally instructed CXCR4^{hi} neutrophils represented early and critical players in the initiation of type 2 allergic asthma against HDM allergens. Given the central role of epithelial-derived alarmins, including IL-33, IL-25 and TSLP in the initiation of type 2 allergic immunity[39], it would be interesting to test their respective contributions to the imprinting of CXCR4^{hi} neutrophils.

We used DNAse, NEi and Cl-amidine to assess the functional importance of NETs in the initiation of allergic asthma. None of these approaches are fully specific for NETs[36]. Cl-amidine inhibits the activity of PAD4, which is implicated in chromatin reorganization and is expressed in many cell types. Treatment with Cl-amidine may lead to decreased activity of citrullinated histone proteins rather than NET impairment[19]. In addition, the biological

activity of the inhibitors may not be optimal in the tissue and could be influenced by factors that are inherent to the experimental models used. However, treatment with DNAse, NEi and Cl-amidine impaired NETs and had the same global outcome on the development of HDM-induced asthma, suggesting that NETs could be mediating the onset of allergic airway inflammation to HDM in the models tested here.

Low-dose LPS, influenza virus infection and ozone exposure were associated with an increased uptake of fluorescent-labelled HDM by CD11b^{+}Ly-6C^{+} DCs, an important step in the initiation of HDM-specific type 2 responses[31,32]. Allergen uptake was significantly reduced in NET-targeted mice, supporting the idea that NETs can directly or indirectly modulate this process. *Ex vivo* co-culture experiments with lung neutrophils and BMDCs further indicated that NETs derived from LPS^{lo} neutrophils could directly promote HDM uptake by CD11b^{+}Ly-6C^{+} DCs. Our study is in accordance with reports that extracellular host DNA, the main NET component, is a potent signal that promotes the activation of DCs and type 2 immune responses[20,40].

Whether CXCR4^{hi} neutrophils and NETs can trigger type 2 sensitization against other type 2-inducing stimuli, such as fungal proteases, food allergens, helminths or additional pro-allergic factors, such as other respiratory viruses, exhaust particles, cigarette smoke, in BALB/c or other genetic backgrounds remains unclear[17]. In humans, neutrophils are important immune-modulating cells in the effector phase of severe asthma, which is characterized by neutrophilic inflammation, high expression of IL-17 and resistance to corticosteroids[16–19]. Whether particular NET-releasing neutrophils contribute to the initiation of type 2 allergic asthma in humans remains unknown. A prospective Danish study found that the number of respiratory infections in early life, but not the particular viral trigger, was associated with asthma development[41]. The authors postulated that a host-derived factor might underlie the increased allergic susceptibility[41]. Our results suggest that the accumulation of NET-prone neutrophils could be such host-associated factor. In addition, blood neutrophils from Hutterite children, who are raised in an environment poor in LPS and are prone to develop allergies, have higher expression of CXCR4 compared to blood neutrophils from Amish children, who live in LPS-rich homes and protected from allergies[38]. While lung neutrophils have not been assessed in these children, it is tempting to speculate that environmental risk factors may promote allergic airway sensitization in humans by inducing NET-prone CXCR4^{hi} neutrophils, which increase host susceptibility to mount type 2 allergic responses towards aeroallergens.

Methods

Mice

Female BALB/c mice were purchased from Janvier Laboratories. Age-matched, 6- to 10-week-old mice were used for experiments. Mice were housed under specific pathogen free (SPF) conditions and maintained in a 12-h light-dark cycle with food and water *ad libitum.* All animal experiments described in this study were reviewed and approved by the Institutional Animal Care and Use Committee of the University of Liège. The "Guide for the Care and Use of Laboratory Animals", prepared by the Institute of Laboratory Animal

Resources, National Research Council, and published by the National Academy Press, as well as European and local legislations, were followed carefully.

Reagents and antibodies

2.4G2 Fc receptor blocking antibodies were produced in house. Anti-mouse FITC- and V500-conjugated anti-CD45.2 (clone 104), PE-conjugated anti-CD3 (clone 142-2C11), PE-conjugated anti-CD19 (clone 1D3), PE-conjugated anti-NK1.1 (clone pk136), PE-conjugated anti-SiglecF (clone E50-2440), PE-conjugated anti-Ly-6G (clone RB6-8C5), eFluor450- and PE-Cy7-conjugated anti-CD11b (clone M1/70), PE-Cy7-conjugated anti-Ly-6G (clone 1A8), APC-Cy7-conjugated anti-CD11c (clone HL3), PE-CF594-conjugated anti-Ly-6C (clone 49-44), FITC-conjugated anti-CD103 (clone M290), PE-conjugated anti-Lamp-1 (CD107a) (clone 1D4B) and PE-conjugated streptavidin antibodies were purchased from BD biosciences. Anti-mouse PE-conjugated anti-CXCR4 (clone 2B11), anti-mouse PE-conjugated anti-CD49d (clone R1-2) and anti-mouse anti-CD86 biotin (clone GL-1) antibodies were purchased from eBioscience. Anti-mouse PerCP-Cy5.5-conjugated anti-MHC-II (Ia-Ie) (clone M5/M4,15,2) and BV421-conjugated anti-CD64 (clone X54-5/7.1) antibodies were purchased from Biolegend.

Unconjugated goat anti-mouse myeloperoxidase (MPO) (cat. AF3667) antibodies were purchased from R&D systems, unconjugated rabbit anti-mouse anti-citrullinated H3 (cat. Ab5103) antibodies were purchased from Abcam. Donkey anti-rabbit and anti-goat IgG antibodies conjugated with AlexaFluor568 and AlexaFluor488, respectively, were purchased from ThermoFisher.

Anti-mouse HSP90α, goat anti-rabbit immunoglobulins/HRP and rabbit anti-mouse immunoglobulins/HRP were purchased from Agilent.

Additional reagents can be found in the sections below.

Model of low-dose-LPS-triggered allergic asthma to HDM

Isoflurane-anesthetized BALB/c wild-type mice were instilled i.n. with different doses of LPS ranging from 0.1 ng to 10 µg, two of which being chosen as low (100 ng) or high (10 µg) doses (LPS from Escherichia coli O55:B5, Sigma-aldrich). Vehicle mice were instilled i.n. with 50 µl PBS. One day later (Day 1), mice were administered i.n. with 40 µg HDM (HDM *pteronyssinus,* Greer Laboratories) in 50 µl PBS. Seven days later (Day 8), all mice were challenged by i.n. instillation of 10 µg HDM in 50 µl PBS. Three days after the HDM challenge (Day 11), we estimated bronchial hyperresponsiveness to methacholine by assessing dynamic airway resistance in anesthetized animals subjected to increased doses of methacholine with a FlexiVent small animal ventilator (SCIREQ) system[42]. Animals were then sacrificed and features of allergic airway inflammation were assessed. BALF cytology and lung histology were performed as described[42]. The extent of perivascular and peribronchial inflammation was estimated by a score calculated by means of quantification of inflammatory cells in lung sections stained with hematoxylin and eosin[43]. Briefly, score 0 was assigned to bronchi with no surrounding leukocyte infiltration; score 1 corresponded to few infiltrating leukocytes; scores 2 or 3 were assigned if there were from 1 to 2, or 3 to 5 layer(s) of perivascular and/or peribronchial leukocytes, respectively. Mucus production was

quantified as the percentage of Periodic Acid Schiff (PAS)–stained goblet cells per total epithelial cells in randomly selected bronchi. Bronchial lymph node (BLN) cells were collected, pooled from 2-5 mice (Figs. 1c, 4j, 5d, 8b,g) and cultured in complete RPMI medium with or without HDM restimulation (30 μg/ml). Culture supernatants were assessed for cytokine production (IL-4, IL-5, IL-13, IFN-γ) by ELISA (eBiosciences).

Cell isolation, staining and flow cytometry

To obtain single-lung-cell suspensions, lungs were perfused with 10 ml of PBS through the right ventricle, cut into small pieces, and digested for 1 h at 37°C in HBSS containing 1 mg/ml collagenase A (Roche) and 0.05 mg/ml DNase I (Roche). Blood was collected in an EDTA-containing tube (100 mM), and red blood cells were lysed with RBC lysis buffer (eBioscience). BM cells were isolated by flushing femurs with PBS. Cells were filtered through a 70μM cell strainer to obtain single cell suspensions.

Cell phenotyping and sorting were performed on a FACSCANTO II and a FACSARIA III (BD Biosciences), respectively. Staining reactions were performed at 4°C with 2% v/v/ of Fc block (BD Pharmingen) to reduce non-specific binding. Anti-mouse Lamp-1 intracellular staining was performed using the Foxp3/Transcription factor Staining Buffer Set from eBiosciences.

FSC-W and FSC-A discrimination was used to exclude doublet cells, and ViaProbe (7-AAD) cell viability solution (BD Biosciences) was used to discriminate between dead and living cells. BM, blood and lung neutrophils were identified as $SSC^{hi}CD45^+CD11b^{hi}Ly$-6G^{hi} cells. Neutrophil Mean Fluorescence Intensity (MFI) of specific markers was quantified using FlowJo. Results were analyzed using FlowJo (Tree Star, Ashland, USA).

For scRNA-seq, adoptive transfer and co-culture experiments, single-lung-cell suspensions were obtained from lungs of vehicle, LPS^{lo} and LPS^{hi} mice 24 h after treatment. Neutrophils were first enriched by negative selection using a magnetic-activated cell sorting (MACS, Neutrophil Isolation kit, Miltenyi Biotec) and then sorted as CD45$^+$ cells using nozzle 100 at 3000 events/second (see Supplementary Fig. 2b,c). Trypan blue-treated cells were examined under the microscope for counting and viability testing. Viability was above 95% for all three samples. Cell preparations were centrifuged at 300g for 5 min. For scRNA-seq, neutrophils were isolated from lung single-cell suspensions pooled from 3 BALB/c female wild-type mice per condition, and were resuspended in calcium- and magnesium-free PBS containing 400μg/ml bovine serum albumin (BSA, Sigma-Aldrich).

For cytologic examination and immunofluorescence *ex vivo*, CD45$^+$CD11b^{hi}Ly-6G^{hi}CD49d^{lo} neutrophils from vehicle and LPS^{hi} mice and CD45$^+$CD11b^{hi}Ly-6G^{hi}CD49d^{hi} neutrophils from LPS^{lo} mice were FACS-sorted 24 h after LPS.

ScRNA-seq: library construction using 10X Genomics® platform

Cellular suspensions were loaded on the Chromium™ Controller (10x Genomics, Pleasanton, CA, USA) in order to generate Gel Bead-In-EMulsions (GEMs). Barcoded

sequencing libraries were generated by using the Chromium™ Single Cell 3' Reagent Kits v2 (10x Genomics, Pleasanton, CA, USA) following manufacturer's instructions. Sequencing libraries were loaded at 1.4 pM on an Illumina NextSeq500 with NextSeq 500/550 Mid Output v2 kit (150 cycles) (Illumina, CA, USA) using the following read lengths: 26 bp for Read1 (16 bp Barcode + 10 bp Randomer), 8 bp for Sample Index and 58 bp for Read2.

Analysis scRNA-seq samples

Cell Ranger software (v1.2.0) (10x Genomics) was used to demultiplex Illumina BCL files to FASTQ files (cellranger mkfastq), to perform alignment (to mouse GRCm38/mm10 genome), filtering, UMI counting and to produce gene – barcode matrices (cellranger count).

Subsequent analysis used R bioconductor[44] (version 3.4.2.), and the R package Seurat[45] (version 2.1.0). We first performed a quality control analysis and selected cells for further analysis (see Supplementary Fig. 2d,e). Gene counts were normalized and highly variable genes were calculated. Cell-cell variation in the number of detected UMI was regressed out using the ScaleData function. Linear dimensional reduction was performed on the scaled data using the 'RunPCA' function. To identify the number of statistically significant principal components (PCs) to include for subsequent analyses, we used the 'JackStraw' function, which implements a resampling test inspired by the jackStraw procedure[45]. PC 1:11 were used in the subsequent analyses. We have also performed analyses including lower and higher numbers of PCs (1:8 to 1:13) and did not find any substantial change in the results obtained. Cells were clustered via the 'FindClusters' function. Several cluster resolutions were tested, and the resolution of 0.25 was chosen, since higher resolutions created additional subdivisions or clusters containing singlets, which were considered not relevant. To visualize the data, non-linear dimensional reduction was used, and *t*SNE plots were created by using the 'RunTSNE' function, with the number of dimensions to use set to 11 (PC 1:11). The aforementioned analyses were performed on the individual Seurat objects (encompassing data from vehicle, LPS^{lo} and LPS^{hi} mice) but also on a merged Seurat object that encompassed merged data from vehicle, LPS^{lo} and LPS^{hi} mice. Differential expression (DE) analysis between clusters was performed using the 'FindMarkers' functionA value of 0.25 was attributed to the min.pct argument, which requires a gene to be detected at least in 25% in either of the two groups of cells. Only DE genes with an adjusted P value $<10^{-3}$ were retained. To define the transcriptomic signature of steady-state neutrophils (cluster 0) (see Supplementary Fig. 3c,d), lists of the significantly upregulated genes in cluster 0 compared to cluster 1 (i.e. LPS^{lo}-induced), cluster 0 compared to clusters 2,3,5 (i.e. LPS^{hi}-induced), and cluster 0 compared to cluster 4 were generated, and genes commonly found in each of the 3 lists were retained. To define the common 'LPS signature' (see Supplementary Fig. 3e,f), lists of the significantly upregulated genes in cluster 1 compared to cluster 0, clusters 2,3,5 compared to 0, and cluster 4 compared to cluster 0 were generated, and genes commonly found in each of the 3 lists were retained. To define cluster-specific gene signatures, only genes that did not belong to the common LPS signature and that were significantly upregulated in that specific cluster as compared to each of the others were retained. Statistical enrichment tests for Gene Ontology (GO) biological processes were performed with PANTHER 13.1 using specific gene set for each cluster with a P value $<10^{-3}$

and minimal detection in 25% of cells with all gene contained in gene ontology *Mus Musculus* database as reference.

Neutrophil cytologic examination

Cytologic examination of FACS-sorted neutrophils was performed on cytospin preparations stained with Hemacolor (Merck KgaA). Sections were examined with a FSX100 microscope (Olympus). Quantifications of neutrophil size and cytoplasm/nucleus ratio were performed using the ImageJ software.

Immunofluorescence

To assess the ability of neutrophils to form NETs *ex vivo*, 2.5 x 10^5 FACS-sorted neutrophils were seeded and cultured *ex vivo* on slides (Nunc® Lab-Tek® II Chamber Slide™ system, Sigma) pre-coated with poly-D-lysin hydrobromide (Sigma) for 24 h in supplemented D-MEM medium (Gibco). Supernatants were removed and chambers were rinsed with PBS. Slides were then fixed with paraformaldehyde 10%, rinsed twice with PBS and permeabilized in PBS 0.5% triton X-100. Slides were then blocked and stained as described below.

To identify NETs from lung tissues, lungs were collected without performing BALF and fixed with 4% paraformaldehyde in PBS. Lung tissues were paraffin-embedded and lung sections were cut (2-μm-thick sections) for immunofluorescence staining. After deparaffinization and rehydration, tissue sections were boiled for 20 min in 10-mM sodium carbonate buffer for antigen retrieval. Lung sections were permeabilized in PBS 0.5% triton X-100.

Samples were incubated with a blocking buffer (PBS with 2% BSA and 2% of donkey serum [Sigma-Aldrich]) for 1 h at room temperature (RT) and stained in blocking buffer with rabbit anti-mouse antibodies directed against citrullinated histone H3 (1:100 in blocking buffer) and with goat anti-mouse antibodies directed against myeloperoxidase (MPO) (1:40 in blocking buffer) during 1 h at RT. After washing samples with PBS, secondary donkey anti-rabbit IgG antibodies conjugated with AlexaFluor568 (1:200 in blocking buffer) and donkey anti-goat IgG antibodies conjugated with AlexaFluor488 (1:200 in blocking buffer) were added in blocking buffer containing DAPI (1:1000) and incubated for 2 h in the dark at RT. Finally, samples were mounted with 10 μl of ProLong Antifade reagent (ThermoFisher) on glass slides and stored at RT in the dark overnight.

All samples were analyzed by fluorescence microscopy using standard filter sets. Controls were stained with secondary antibody only, and nonspecific fluorescent staining was not detected when secondary antibodies were tested alone. Images were acquired on a Zeiss LSM 880 Airyscan Elyra S.1. confocal microscope (Zeiss) and processed using the ImageJ software. To quantify the volume of NETs released by neutrophils *ex vivo* (see Supplementary Fig. 4g) or present in the lung tissue (see Figs. 3j,k; 5a,b; 7i,m; Supplementary Figs. 5g; 6b; 7j), Z stack pictures were acquired and Imaris software was used. Briefly, we performed a three-dimensional (3D) reconstruction of structures staining double positive for H3-Cit (red) and MPO (green), and Imaris provided quantification of the volume of these structures, expressed as mm^3 per 10^2 neutrophils for *ex vivo* experiments

(counted under the bright-field microscope and staining positive for intracellular MPO associated with the granules) or per 10^2 mm^3 of lung tissue.

DsDNA measurement in BALF

DsDNA was measured in the acellular fraction of the BALF, which was obtained after a double centrifugation and supernatant collection. Levels of dsDNA were determined using Quant-iT PicoGreen dsDNA reagent (Invitrogen, Carlsbad, CA) according to the manufacturer's protocol.

Western blotting

Lung tissues were homogenized in RIPA buffer supplemented with a cocktail of protease inhibitors (Complete, Roche). An equivalent amount of protein per sample was resolved on a 4-20% gel (Mini-PROTEAN® TGX™ Precast Gels, biorad) and electroblotted on Invitrolon PVDF membranes (Life technologies). Membranes were blocked 1 h at RT in TBS-Tween 0.1% containing 5% of dry milk and incubated overnight at 4°C with primary antibody anti-citrullinated H3 (1:1000 in TBS-tween 0.1% and BSA 5%). The membranes were then incubated 2 h at RT with appropriate HRP-associated secondary antibodies in TBS-tween 0.1% containing 5% BSA. Equal loading was confirmed by probing for HSP90α.

Measurement of NE/DNA complexes in BALF

Nunc plates (ThermoFisher) were coated overnight with anti-NE antibodies (1/2000, Abcam, ab21595) and washed 3 times with PBS-Tween 0.05%. Plates were blocked 1 h at RT with PBS-BSA 1% and washed 3 times. Samples were then loaded for 2 h at RT and plates were then washed 5 times. Mouse anti-dsDNA antibodies were added for 1 h at RT followed, after 5 washes, by incubation with biotinylated rat anti-mouse IgG polyclonal antibodies for 90 min at RT. After extensive washing, secondary streptavidin-HRP (BD pharmingen, cat.554066) was added for 30 minutes at RT, followed by 5 washes. The relative amount of NE/DNA complexes was revealed using TMB substrate solution (Sigma-Aldrich).

Antibody-mediated neutrophil *in vivo* depletion

Neutrophils were depleted by i.p. injection of 500 μg of anti-Ly-6G antibody (*InVivo* Plus anti-mouse Ly-6G, clone 1A8, Bioxcell) intraperitoneally (i.p.) one day before (day -1), at day 0 and one day after LPS exposure (day 1) (see Supplementary Fig. 5a). Mice were sacrificed 3 h later.

Inhibition of LPS-induced lung neutrophil recruitment

To inhibit LPS-induced lung neutrophil recruitment[46], an antagonist of the chemokine receptor CXCR2 (i.e., Sch527123[47], MedChem Express) was given orally, by gavage, at the dose of 3mg/kg, 2 h before, 4 h after and 8 h after LPS treatment, as well as 2 h before and 4 h after i.n. administration of 40 μg HDM. Seven days later, mice were challenged with 10 μg HDM and features of allergic airway inflammation were assessed 3 days later.

Neutrophil adoptive transfers

After MACS enrichment and FACS sorting, neutrophils were resuspended in calcium- and magnesium-free PBS at the concentration of 2.10^7 cells/ml. Five hundred thousand (5×10^5) cells, together with 40 μg HDM, were injected intratracheally to naive mice in 50 μl PBS. Seven days later, mice were challenged with 10 μg HDM and features of allergic airway inflammation were assessed 3 days later.

Degradation of NETs and inhibition of NET formation *in vivo*

The formation of NETs was prevented *in vivo* by i.p. injection of NEi (GW-311616 hydrochloride, Axon Medchem) (2.5μg/g in 200 μl PBS) or of Cl-amidine (10x stock solution in DMSO, Sanbio) (10mg/kg in 200 μl 1% DMSO v/v in PBS), twice daily from day -1 to day +2 (LPS model) or from day 5 to day 17 (PR8 infection model), or from day 0 to day 3 (ozone model). Alternatively, NETs were degraded by injecting 1000 I.U DNAse I (Sigma-Aldrich) i.p. in 200 μl HBSS once daily from day -1 to day +2 (model of LPS exposure) or from day 5 to day 17 (PR8 infection model) or from day 0 to day 3 (ozone model). In pilot experiments, we compared the responses of LPS[lo]/HDM, PR8/HDM or ozone/HDM mice with their vehicle-treated counterparts (either HBSS, PBS or 1% DMSO v/v, used separately) and confirmed that vehicle did not affect the response. In subsequent experiments, vehicle LPS[lo]/HDM, PR8/HDM or ozone/HDM mice were treated randomly with either HBSS, PBS or DMSO 1% v/v.

AF647-HDM uptake by lung DC subsets

To assess HDM uptake by lung DCs, LPS[lo] or ozone-exposed mice were administered i.n. with 40 μg of HDM labelled with Alexafluor-647 (AF647-HDM) (Alexa Fluor™ 647 Protein Labeling Kit, ThermoFisher) 24 h after treatment. Alternatively, PR8-infected mice were injected i.n. with AF647-HDM at day 7 post-infection. Twenty-four h later, lung-single-cell suspensions were obtained and lung dendritic cells (DCs) were selected as CD45^{+}CD3e^{-}CD19^{-}SiglecF^{-}Ly-6G^{-}NK1.1^{-}MHC-II^{+}CD11c^{+} cells and were then subdivided into CD11b^{-}CD103^{+}, CD11b^{+}Ly-6C^{-} and CD11b^{+}Ly-6C^{+} subsets by flow cytometry (see Fig. 6a). Alternatively, mice were also treated with NEi, Cl-amidine or DNAse as described above.

Neutrophils/BMDCs co-culture experiments

To generate BMDCs, BM cells were isolated from naive BALB/c mice and were grown for 7 days in GM-CSF-containing medium, as described[48]. Vehicle, LPS[lo] and LPS[hi] neutrophils were isolated 24 h after treatment. Two hundred fifty thousand (2.5×10^5) neutrophils were seeded into 48 wells plates previously coated with poly-D-lysin hydrobromide (Sigma) in supplemented D-MEM medium (Gibco) and allowed to adhere for 2 h. BMDCs were then added to neutrophil cultures at a ratio of 1:1. Finally, AF647-HDM (500 ng/ml) and DNAse I (400 I.U./ml, Sigma-Aldrich) were added to the culture. Twelve h later, cells were collected, washed, resuspended in FACS medium and stained for flow cytometry analysis.

Influenza A virus infection protocol

Influenza A virus strain A/PR8/34 (H1N1) was kindly provided by F. Trottein (Institut Pasteur, Lille, France). The viral stock suspension (10^8 PFU/ml) was diluted and 5 PFU were administered i.n. to isoflurane-anesthetized mice in 50 μl PBS.

Assessment of viral mRNA expression

Lung apical lobes were excised and total mRNA was isolated from homogenized tissue according to the Immgen protocol (www.immgen.org). cDNA was obtained using RevertAid First Strand cDNA Synthesis Kit (ThermoFisher Scientific) and qPCR was performed in duplicate using iTaq Universal SYBR geen supermix (Biorad) and ABI 7900HT Fast Real-Time PCR System (Applied Biosystems). Primer sequences were as followed: *5'-TTCACCATTGCCTTCTCTTC-3'* and *5'-CCCATTCTCATTACTGCTTC-3'* for viral NS1, *5'-AGCCCAGTGTTACCACCAAG-3'* and *5'-ACCCAAGAACAAGCACAAGG-3'* for housekeeping gene *Ubc*, *5'-TGGCAAAGTGGAGATTGTTGCC-3'* and *5'-AAGATGGTGATGGGCTTCCCG-3'* for housekeeping gene *Gapdh*, *5'-CATGGCTCGCTCGGTGACC-3'* and *5'-AATGTGAGGCGGGTGGAACTG-3'* for housekeeping gene *B2m*. Expression levels of NS1 were normalized relative to the three control genes (*Ubc, B2m* and *Gapdh*).

Model of PR8-triggered allergic asthma to HDM

Seven days post-infection, mice were administered i.n. with 40 μg HDM. Seven days later (Day 7), all mice were challenged by i.n. instillation of 10 μg HDM. Three days after the challenge, animals were sacrificed and features of allergic airway inflammation were assessed, as described above. In addition, levels of HDM-specific IgG1 were quantified, as described[49].

Model of ozone-triggered allergic asthma to HDM

Naive mice were exposed for 3 consecutive days to 2 ppm ozone during 3 h. Twenty-four h after the last ozone exposure, mice were administered i.n. with 40 μg HDM. Seven days later, mice were challenged with 10 μg HDM and features of allergic airway inflammation were assessed 3 days later as described above.

Statistical analysis

Respect of the assumptions of normal distribution of residuals and homoscedasticity was verified, and data were presented as mean + s.e.m., as well as individual values, unless otherwise indicated. Data from independent experiments were pooled for analysis in each data panel, unless otherwise indicated. Statistical analyses were performed using Prism 6 (GraphPad Software). We considered a *P*-value lower than 0.05 as significant. */°, $P < 0.05$; **/°°, $P < 0.01$, ***/°°°, $P < 0.001$; ns, not significant.

Supplementary Material

Refer to Web version on PubMed Central for supplementary material.

Acknowledgements

Data Availability

The scRNA-seq data provided in this manuscript have been deposited in the ArrayExpress database at EMBL-EBI (https://www.ebi.ac.uk/arrayexpress/experiments/E-MTAB-6902) under accession number E-MTAB-6902. The figures that have associated scRNA-seq data are the following: Fig. 2, Supplementary Figs. 2,3. The source data underlying Figs 1a-d and f; 2d; 3b,c,f,g,i,k; 4b-e, g, i-k and m; 5b-e and g; 6b, d and f; 7 b-i and k-m; 8a-c,e and f-h and j and Supplementary Figs 1b,d; 4c,d; 5 b,c and e,g; 6b, 7b-d,f,g,i,j; 8a are provided as a Source Data file. Any data that support the findings of this study are available from the corresponding authors upon request.

References

1. Braman SS. The global burden of asthma. Chest. 2006; 130:4s–12s. [PubMed: 16840363]

2. Galli SJ, Tsai M, Piliponsky AM. The development of allergic inflammation. Nature. 2008; 454:445–54. [PubMed: 18650915]

3. Vercelli D. Discovering susceptibility genes for asthma and allergy. Nat Rev Immunol. 2008; 8:169–82. [PubMed: 18301422]

4. Eder W, Ege MJ, von Mutius E. The asthma epidemic. N Engl J Med. 2006; 355:2226–35. [PubMed: 17124020]

5. Platts-Mills TA. The allergy epidemics: 1870-2010. J Allergy Clin Immunol. 2015; 136:3–13. [PubMed: 26145982]

6. Busse WW, Lemanske RF Jr, Gern JE. Role of viral respiratory infections in asthma and asthma exacerbations. Lancet. 2010; 376:826–34. [PubMed: 20816549]

7. Peden DB. The epidemiology and genetics of asthma risk associated with air pollution. J Allergy Clin Immunol. 2005; 115:213–9. [PubMed: 15696070]

8. Braun-Fahrlander C, et al. Environmental exposure to endotoxin and its relation to asthma in school-age children. N Engl J Med. 2002; 347:869–77. [PubMed: 12239255]

9. Strachan DP. Family size, infection and atopy: the first decade of the 'hygiene hypothesis'. Thorax. 2000; 55(Suppl 1):S2–10. [PubMed: 10943631]

10. Lloyd CM, Snelgrove RJ. Type 2 immunity: Expanding our view. Sci Immunol. 2018; 3

11. Lambrecht BN, Hammad H. The immunology of asthma. Nat Immunol. 2015; 16:45–56. [PubMed: 25521684]

12. Gregory LG, Lloyd CM. Orchestrating house dust mite-associated allergy in the lung. Trends Immunol. 2011; 32:402–11. [PubMed: 21783420]

13. Locksley RM. Asthma and allergic inflammation. Cell. 2010; 140:777–83. [PubMed: 20303868]

14. Ng LG, Ostuni R, Hidalgo A. Heterogeneity of neutrophils. Nat Rev Immunol. 2019; 19:255–265. [PubMed: 30816340]

15. Papayannopoulos V. Neutrophil extracellular traps in immunity and disease. Nat Rev Immunol. 2018; 18:134–147. [PubMed: 28990587]

16. Krishnamoorthy N, et al. Neutrophil cytoplasts induce TH17 differentiation and skew inflammation toward neutrophilia in severe asthma. Sci Immunol. 2018; 3

17. Radermecker C, Louis R, Bureau F, Marichal T. Role of neutrophils in allergic asthma. Curr Opin Immunol. 2018; 54:28–34. [PubMed: 29883877]

18. Wang YH, Wills-Karp M. The potential role of interleukin-17 in severe asthma. Curr Allergy Asthma Rep. 2011; 11:388–94. [PubMed: 21773747]

19. Lachowicz-Scroggins ME, et al. Extracellular DNA, Neutrophil Extracellular Traps, and Inflammasome Activation in Severe Asthma. Am J Respir Crit Care Med. 2019; 199:1076–1085. [PubMed: 30888839]

20. Toussaint M, et al. Host DNA released by NETosis promotes rhinovirus-induced type-2 allergic asthma exacerbation. Nat Med. 2017; 23:681–691. [PubMed: 28459437]

21. Eisenbarth SC, et al. Lipopolysaccharide-enhanced, toll-like receptor 4-dependent T helper cell type 2 responses to inhaled antigen. J Exp Med. 2002; 196:1645–51. [PubMed: 12486107]

22. Schuijs MJ, et al. Farm dust and endotoxin protect against allergy through A20 induction in lung epithelial cells. Science. 2015; 349:1106–10. [PubMed: 26339029]

23. Zheng GX, et al. Massively parallel digital transcriptional profiling of single cells. Nat Commun. 2017; 8

24. Remijsen Q, et al. Neutrophil extracellular trap cell death requires both autophagy and superoxide generation. Cell Res. 2011; 21:290–304. [PubMed: 21060338]

25. Adrover JM, Nicolas-Avila JA, Hidalgo A. Aging: A Temporal Dimension for Neutrophils. Trends Immunol. 2016; 37:334–45. [PubMed: 27083489]

26. Casanova-Acebes M, et al. Rhythmic modulation of the hematopoietic niche through neutrophil clearance. Cell. 2013; 153:1025–35. [PubMed: 23706740]

27. Dwyer MP, et al. Discovery of 2-hydroxy-N,N-dimethyl-3-{2-[[(R)-1-(5- methylfuran-2-yl)propyl]amino]-3,4-dioxocyclobut-1-enylamino}benzamide (SCH 527123): a potent, orally bioavailable CXCR2/CXCR1 receptor antagonist. J Med Chem. 2006; 49:7603–6. [PubMed: 17181143]

28. Reutershan J, et al. Critical role of endothelial CXCR2 in LPS-induced neutrophil migration into the lung. J Clin Invest. 2006; 116:695–702. [PubMed: 16485040]

29. Cools-Lartigue J, et al. Neutrophil extracellular traps sequester circulating tumor cells and promote metastasis. J Clin Invest. 2013; doi: 10.1172/JCI67484

30. Wang Y, et al. Histone hypercitrullination mediates chromatin decondensation and neutrophil extracellular trap formation. J Cell Biol. 2009; 184:205–13. [PubMed: 19153223]

31. Mesnil C, et al. Resident CD11b(+)Ly6C(-) lung dendritic cells are responsible for allergic airway sensitization to house dust mite in mice. PloS one. 2012; 7:e53242. [PubMed: 23300898]

32. Plantinga M, et al. Conventional and monocyte-derived CD11b(+) dendritic cells initiate and maintain T helper 2 cell-mediated immunity to house dust mite allergen. Immunity. 2013; 38:322–35. [PubMed: 23352232]

33. Marichal T, et al. Interferon response factor 3 is essential for house dust mite-induced airway allergy. J Allergy Clin Immunol. 2010; 126:836–844 e13. [PubMed: 20673978]

34. Larché M, et al. Costimulation through CD86 is involved in airway antigen-presenting cell and T cell responses to allergen in atopic asthmatics. J Immunol. 1998; 161:6375–6382. [PubMed: 9834128]

35. Janss T, et al. Interferon response factor-3 promotes the pro-Th2 activity of mouse lung CD11b+ conventional dendritic cells in response to house dust mite allergens. Eur J Immunol. 2016; 46:2614–2628. [PubMed: 27546168]

36. Al-Garawi AA, et al. Acute, but not resolved, influenza A infection enhances susceptibility to house dust mite-induced allergic disease. J Immunol. 2009; 182:3095–104. [PubMed: 19234206]

37. Hollingsworth JW, et al. Ozone activates pulmonary dendritic cells and promotes allergic sensitization through a Toll-like receptor 4-dependent mechanism. J Allergy Clin Immunol. 2010; 125:1167–70. [PubMed: 20394980]

38. Stein MM, et al. Innate Immunity and Asthma Risk in Amish and Hutterite Farm Children. N Engl J Med. 2016; 375:411–421. [PubMed: 27518660]

39. Roan F, Obata-Ninomiya K, Ziegler SF. Epithelial cell-derived cytokines: more than just signaling the alarm. J Clin Invest. 2019; 129:1441–1451. [PubMed: 30932910]

40. Marichal T, et al. DNA released from dying host cells mediates aluminum adjuvant activity. Nat Med. 2011; 17:996–1002. [PubMed: 21765404]

41. Bonnelykke K, Vissing NH, Sevelsted A, Johnston SL, Bisgaard H. Association between respiratory infections in early life and later asthma is independent of virus type. J Allergy Clin Immunol. 2015; 136:81–86 e4. [PubMed: 25910716]

42. Sabatel C, et al. Exposure to Bacterial CpG DNA Protects from Airway Allergic Inflammation by Expanding Regulatory Lung Interstitial Macrophages. Immunity. 2017; 46:457–473. [PubMed: 28329706]

43. Janss T, et al. Interferon response factor-3 promotes the pro-Th2 activity of mouse lung CD11b+ conventional dendritic cells in response to house dust mite allergens. Eur J Immunol. 2016; 46:2614–2628. [PubMed: 27546168]

44. Gentleman RC, et al. Bioconductor: open software development for computational biology and bioinformatics. Genome Biol. 2004; 5:R80. [PubMed: 15461798]

45. Macosko EZ, et al. Highly Parallel Genome-wide Expression Profiling of Individual Cells Using Nanoliter Droplets. Cell. 2015; 161:1202–1214. [PubMed: 26000488]

46. Reutershan J, et al. Critical role of endothelial CXCR2 in LPS-induced neutrophil migration into the lung. J Clin Invest. 2006; 116:695–702. [PubMed: 16485040]

47. Dwyer MP, et al. Discovery of 2-hydroxy-N,N-dimethyl-3-{2-[[(R)-1-(5- methylfuran-2-yl)propyl]amino]-3,4-dioxocyclobut-1-enylamino}benzamide (SCH 527123): a potent, orally bioavailable CXCR2/CXCR1 receptor antagonist. J Med Chem. 2006; 49:7603–6. [PubMed: 17181143]

48. Marichal T, et al. Interferon response factor 3 is essential for house dust mite-induced airway allergy. J Allergy Clin Immunol. 2010; 126:836–844 e13. [PubMed: 20673978]

49. Toussaint M, et al. Host DNA released by NETosis promotes rhinovirus-induced type-2 allergic asthma exacerbation. Nat Med. 2017; 23:681–691. [PubMed: 28459437]
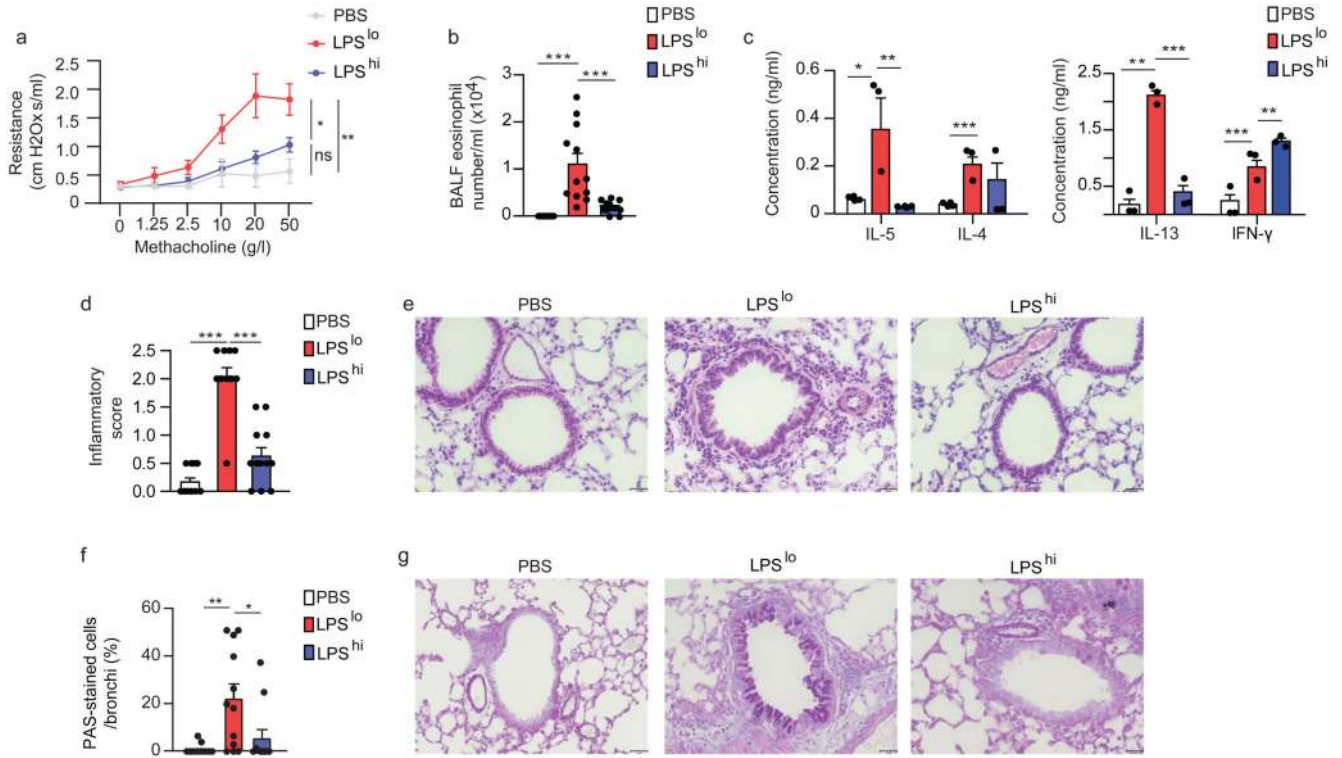
Figure 1. Pre-exposure to low-dose LPS potentiates HDM-induced type 2 allergic asthma.
a, Invasive measurement of dynamic airway resistance upon methacholine inhalation showing bronchial hyperreactivity in vehicle-HDM, LPS^{lo}-HDM and LPS^{hi}-HDM mice, assessed 3 days after the second HDM administration. **b**, Eosinophil cell counts in the BALF of mice, as in a. **c**, ELISA measurement of cytokine production by HDM-restimulated bronchial lymph node (BLN) cells of mice as in a. **d,** Inflammatory score estimating perivascular and peribronchial inflammation, quantified from H&E-stained lung sections of mice as in a. **e**, Representative H&E staining of lung sections of mice as in a. **f**, Quantification of PAS-stained epithelial cells per bronchi showing airway mucus production in mice as in a. **g**, Representative PAS staining of lung sections of mice as in a. (**a-d,f**) Data show mean + s.e.m. and are pooled from (**a**) 2 independent experiments (n=6 mice/group) or (**b-d,f**) ⩾3 independent experiments, each symbol representing (**b,d,f**) individual mice (n=12/group) or (**c**) independent experiments in which cells from 4 mice were pooled by group. *P* values were calculated using (**a**) a mixed effects model with Geisser greenhouse correction or (**b-d,f**) a one-way ANOVA with Tukey's *post hoc* test. *P<0.05; **P<0.01; ***P<0.001. BALF, bronchoalveolar lavage fluid; ns, not significant i.n., intranasal(ly). Scale bar = 32 µm.
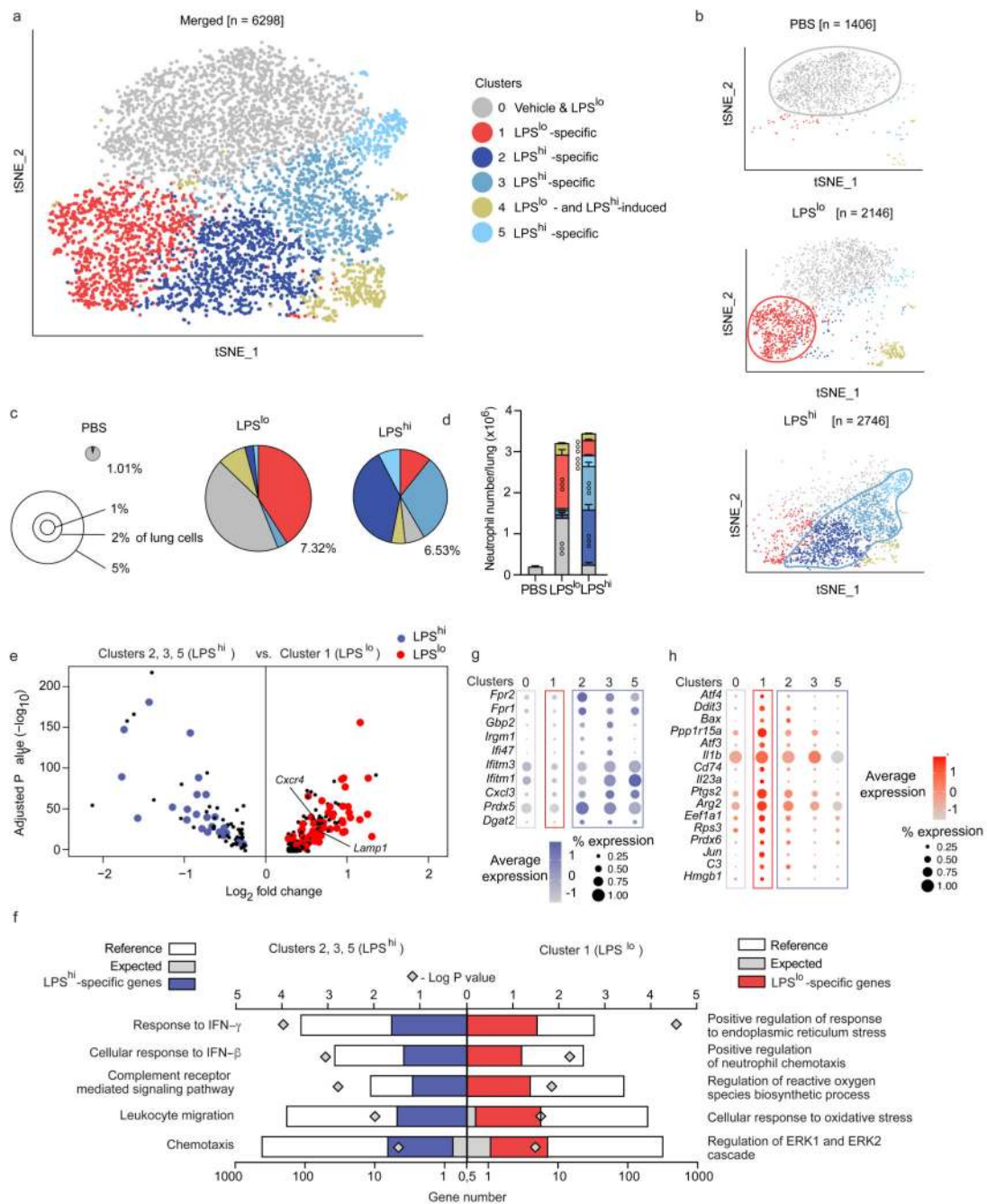
Figure 2. ScRNA-seq analysis of the lung neutrophil compartment 24 h after pro-allergic low or protective high LPS exposure.

a, *t*SNE plots depicting the transcriptional identity of lung neutrophils merged from vehicle, LPS^lo and LPS^hi mice 24 h after treatment, analyzed by scRNA-seq (n=3 pooled mice/ group). **b**, *t*SNE plots depicting the transcriptional identity of lung neutrophils from the three separate experimental conditions as in a. **c**, Pie charts depicting the relative contribution of each neutrophil cluster to the pool of neutrophils in lungs of mice as in a. Insets indicate average percentage of neutrophils among total lung cells. **d**, Absolute numbers of lung

neutrophils per cluster in mice as in a. **e**, Volcano plot depicting the differentially expressed genes between LPS^{hi} and LPS^{lo} lung neutrophils of mice as in a. Transcripts characteristic of the common LPS, the LPS^{lo}- and LPS^{hi}-specific signatures are colored in black, red and blue, respectively. **f**, PANTHER GO enrichment tests on the genes of the LPS^{hi} (left) and LPS^{lo} (right) signatures. **g-h**, Dot plots showing average expression of genes of the (**g**) LPS^{hi} and (**h**) LPS^{lo} signatures within neutrophil clusters. Data in (**d**) show mean + s.e.m. (n=3 mice/group). *P* values were calculated using (**d**) a two-way ANOVA with Tukey's *post hoc* test, (**e**) a likelihood ratio test based on zero-inflated data to identify positive and negative markers of a single cluster compared to some or all other clusters or (**f**) a two-tailed Mann-Whitney U test with Benjamini-Hochberg False Discovery Rate (FDR) correction. The symbol ° within a given cluster in d indicates that neutrophil numbers in that cluster are significantly different from the ones of the same cluster in the two other experimental conditions. °°°*P*<0.001. GO, Gene Ontology.
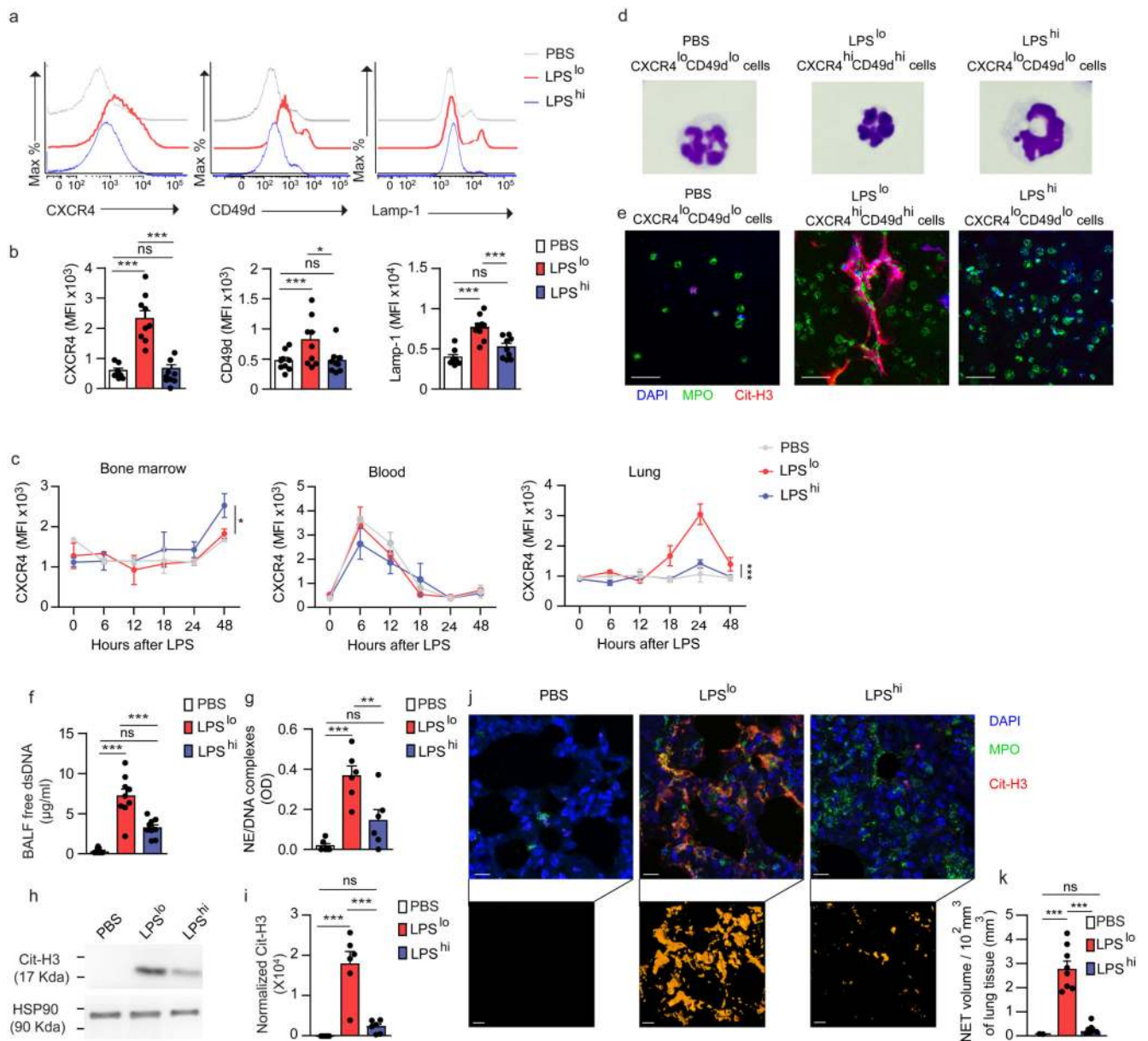
Figure 3. Pro-allergic low-dose LPS instructs lung neutrophils to upregulate CXCR4, CD49d and Lamp-1 and release NETs.

a, Representative histograms of CXCR4, CD49d and Lamp-1 expression by lung CD45$^+$CD11b$^+$Ly-6G$^+$ neutrophils from vehicle, LPS^{lo} and LPS^{hi} mice 24 h after treatment. **b**, MFI showing quantification of CXCR4, CD49d and Lamp-1 expression by lung CD45$^+$CD11bhi$^{Ly-6Ghi}$neutrophils as in a. **c**, Kinetic analysis of CXCR4 expression by bone marrow, blood and lung CD45$^+$CD11b$^+$Ly-6G$^+$ neutrophils from mice as in a. **d**, Representative photographs of FACS-sorted CXCR4^{lo}CD49d^{lo}, CXCR4^{lo}CD49d^{lo} and CXCR4^{hi}CD49d^{hi} lung neutrophils from mice as in a. **e**, Confocal microscopy stainings of Cit-H3$^+$MPO$^+$DAPI$^+$ NETs released from *ex vivo*-cultured neutrophils as in d. Pictures are representative of one of 4 independent sorting experiments. **f**, Levels of extracellular dsDNA

in the BALF of vehicle, LPS^{lo} and LPS^{hi} mice 24 h after treatment. **g**, ELISA measurement of NE/DNA complexes in the BALF of mice as in f. **h**, Representative blots of Cit-H3 and HSP90α (loading control) assessed by Western blot of lung protein extracts from mice as in f. **i**, Quantification of normalized Cit-H3 levels in lung protein extracts of mice as in f. **j**, Confocal microscopy stainings (top) and three-dimensional modeling (bottom) of Cit-H3$^+$MPO$^+$ NETs on lung sections of mice as in f. Pictures are representative of one of >6 lungs analyzed. **k**, Quantification of NET volume in lung sections of mice as in f (n= 8 mice/ group). Data show mean + s.e.m and are pooled from (**b,f,g,i**) 3 independent experiments (b,f,g,i: n=9,9,6,6 mice/group, respectively), or (**c**) 2 independent experiments perand to release neutrophil extracellular traps time point analyzed (n=3 mice/time point). *P* values were calculated using a one-way ANOVA with Tukey's *post hoc* test. *P<0.05; **P<0.01; ***P<0.001. *P* values compare LPS^{lo} vs. vehicle or LPS^{hi} mice in c (i.e., treatment effect). BALF, bronchoalveolar lavage fluid; OD, optical density; ns, not significant. Scale bar = 10 μm.
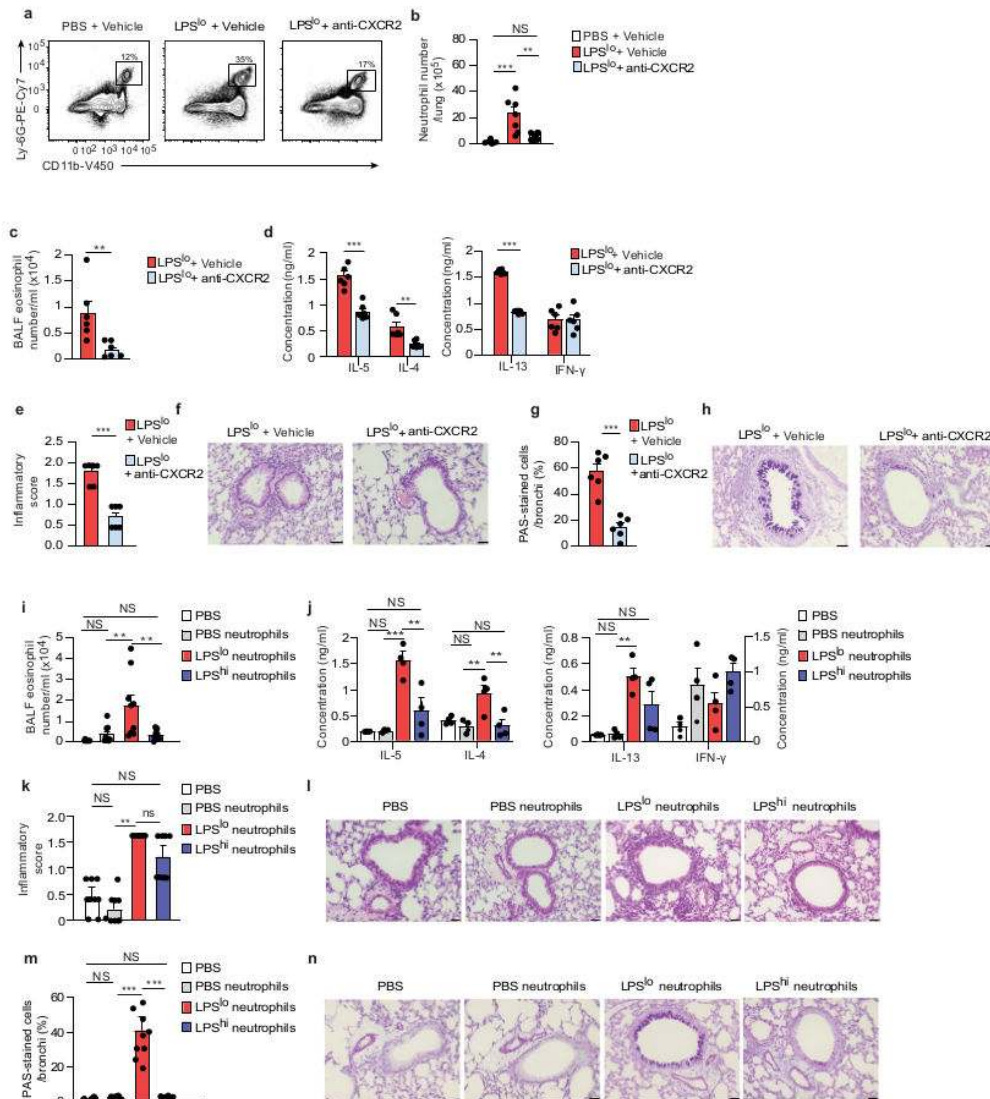
Figure 4. LPS^{lo} neutrophils mediate susceptibility to HDM-induced type 2 allergic airway inflammation.

a, Representative dot plots of lung CD45$^+$CD11b$^+$Ly-6G$^+$ neutrophils from vehicle or LPS^{lo} mice treated or not with Sch527123, a CXCR2 antagonist (anti-CXCR2), 2 h before and 4, 8 and 20 h after LPS, and analyzed 24 h after LPS^{lo}. Insets indicate % of cells within the gate. **b**, Absolute numbers of lung CD45$^+$CD11b$^+$Ly-6G$^+$ neutrophils as in a. **c**, Eosinophil cell counts in the BALF, assessed 3 days after the second HDM administration in LPS^{lo}-HDM mice treated or not with anti-CXCR2, 2 h before and 4 and 8 h after LPS^{lo}, and 2 h before

and 4 h after i.n.sensitization with HDM. **d**, ELISA measurement of cytokine production by HDM-restimulated BLN cells of mice as in c. **e**, Inflammatory score estimating perivascular and peribronchial inflammation, quantified from H&E-stained lung sections of mice as in c. **f**, Representative H&E staining of lung sections of mice as in c. **g**, Quantification of PAS-stained epithelial cells per bronchi showing airway mucus production in mice as in c. **h**, Representative PAS staining of lung sections of mice as in c. **i**, Eosinophil cell counts in the BALF, assessed 3 days after the second HDM administration in mice transferred i.t. with vehicle, LPS^{lo} and LPS^{hi} neutrophils and exposed to HDM. **j**, ELISA measurement of cytokine production by HDM-restimulated BLN cells of mice as in i. **k**, Inflammatory score estimating perivascular and peribronchial inflammation, quantified from H&E-stained lung sections of mice as in i. **l**, Representative H&E staining of lung sections of mice as in i. **m**, Quantification of PAS-stained epithelial cells per bronchi showing airway mucus production in mice as in i. **n**, Representative PAS staining of lung sections of mice as in i. **(b-e,g,i-k,m)** Data show mean + s.e.m. and are pooled from (**b-e,g**) 2 independent experiments, each symbol representing individual mice (n=6/group) or (**i-k,m**) ≥3 independent experiments, each symbol representing (**i,k,m**) individual mice (n=9/group) or (**j**) independent experiments in which cells from 2-3 mice were pooled by group. *P* values were calculated using using a (**b,i-k,m**) one-way ANOVA with Tukey's *post hoc* test, (**c**) a two-sided unpaired Student's *t* test or (**d-e,g**) a two-sided Mann-Whitney test. *P<0.05; **P<0.01; ***P<0.001. ns, not significant. BALF, bronchoalveolar lavage fluid. i.t., intra-tracheal ns, not significant. Scale bar = 32 μm.
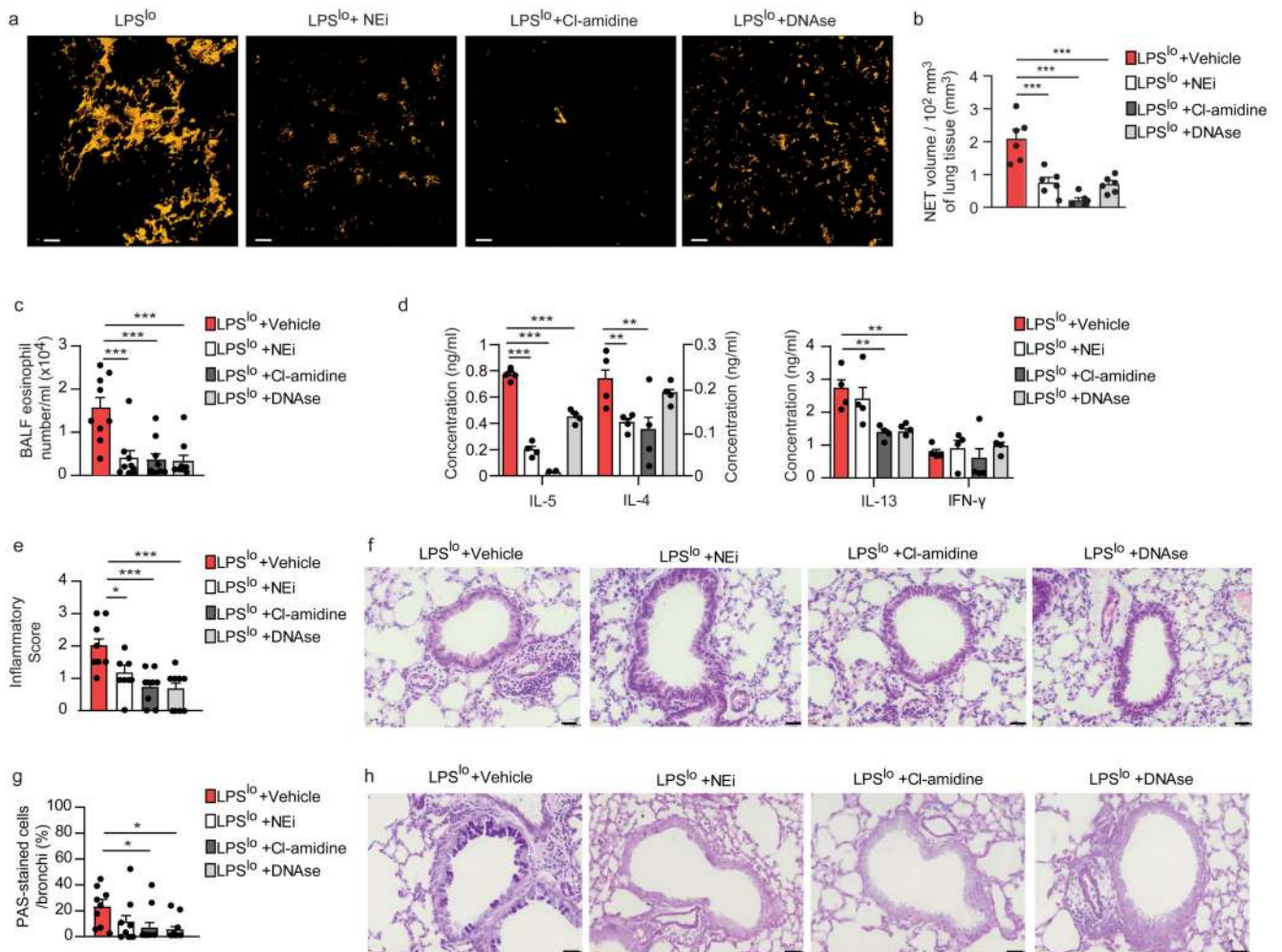
Figure 5. NETs mediate low-dose-LPS-triggered type 2 allergic airway inflammation to HDM.
a, Three-dimensional modeling of Cit-H3$^+$MPO$^+$ NETs on lung sections, assessed 24 h after LPS^{lo} in mice treated i.p. with DNAse one day before and at the time of LPS^{lo} treatment, or treated 4 times i.p. with NEi or Cl-amidine, every 12 h starting one day before LPS^{lo}. Pictures are representative of one of 6 lungs analyzed. **b**, Quantification of NET volume in lung sections of mice as in a. **c**, Eosinophil cell counts in the BALF, assessed 3 days after the second HDM administration in LPS^{lo}-HDM mice treated i.p. with 4 daily injections of DNAse, starting one day before LPS^{lo} treatment, or treated with 8 i.p. injections of NEi or Cl-amidine, every 12 hours starting one day before LPS^{lo} treatment. **d**, ELISA measurement of cytokine production by HDM-restimulated BLN cells of mice as in c. **e**, Inflammatory score estimating perivascular and peribronchial inflammation, quantified from H&E-stained lung sections of mice as in c. **f**, Representative H&E staining of lung sections of mice as in c. **g**, Quantification of PAS-stained epithelial cells per bronchi showing airway mucus production in mice as in c. **h**, Representative PAS staining of lung sections of mice as in c. (**b**) Data show mean + s.e.m. as well as individual mice (n=6/group). (**c-e,g**) Data show mean + s.e.m. and are pooled from 3-4 independent experiments, each symbol representing (**c,e,g**) individual mice (n=9/group) or (**d**) independent experiments in which cells from 2-3

mice were pooled by group. *P* values were calculated using a one-way ANOVA with Tukey's *post hoc* test. *P<0.05; **P<0.01; ***P<0.001. BALF, bronchoalveolar lavage fluid ns, not significant. Scale bars = (**a**) 10 μm; (**f,h**) 32 μm.
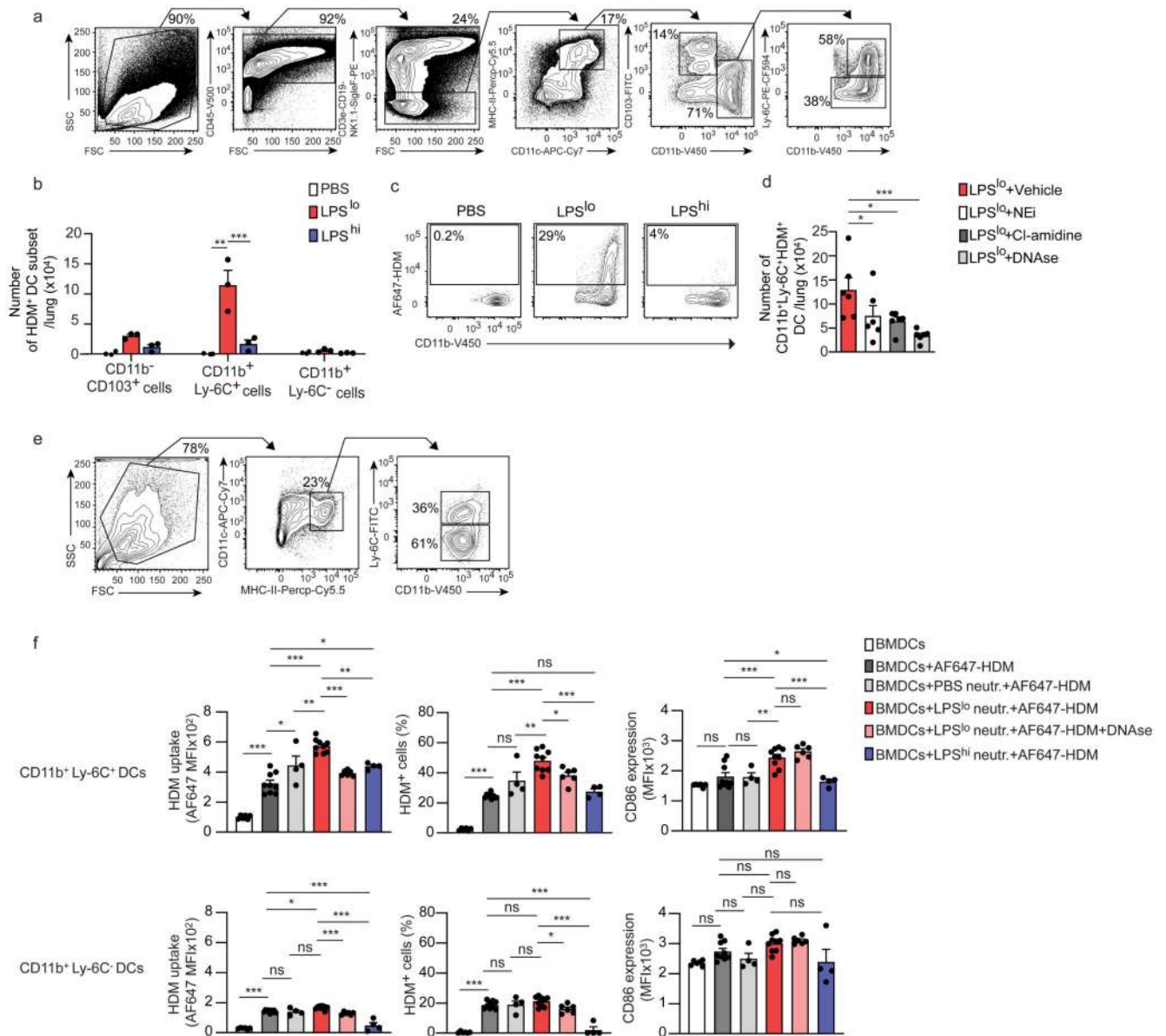
Figure 6. NETs released by LPS^lo neutrophils directly promote HDM uptake by CD11b⁺Ly-6C⁺ DCs.

a, Representative gating strategy delineating lung DC subsets in vehicle-AF647-HDM, LPS^lo-AF647-HDM and LPS^hi-AF647-HDM mice, assessed 24 h after i.n. AF647-HDM. Lung cells from a LPS^lo-AF647-HDM mouse is shown. DCs were defined as CD45⁺CD3e⁻CD19⁻NK1.1⁻SiglecF⁻MHC-II⁺CD11c⁺ cells and further divided into CD11b⁻CD103⁺, CD11b⁺Ly-6C⁻ and CD11b⁺Ly-6C⁺ DCs. **b**, Absolute numbers of lung AF647-HDM⁺ DC subsets in mice as in a. **c**, Representative dot plots showing AF647-HDM MFI in lung CD11b⁺Ly-6C⁺ DCs from mice as in a. **d**, Absolute numbers of lung CD11b⁺Ly-6C⁺AF647-HDM⁺ DCs, assessed 24 h after i.n. AF647-HDM in LPS^lo-AF647-HDM mice treated i.p. with 3 daily injections of DNAse, starting one day before LPS^lo treatment, or treated with 5 i.p. injections of NEi or Cl-amidine, every 12 h starting one day before LPS^lo

treatment. **e**, Representative gating strategy delineating BMDC subsets. BMDCs were defined as MHC-II$^+$CD11c$^+$ cells and further divided into CD11b$^+$Ly-6C$^-$ and CD11b $^+$Ly-6C$^+$ subsets. **f**, MFI of AF647-HDM (left), % of AF647-HDM$^+$ cells (middle), and CD86 expression in CD11b$^+$Ly-6C$^+$ (top) and CD11b$^+$Ly-6C$^-$ (bottom) BMDCs, assessed 12 h after treatment with AF647-HDM and after co-culture with vehicle, LPS^{hi} or LPS^{lo} neutrophils in the presence or absence of DNAse. (**b,d,f**) Data show mean + s.e.m. and are pooled from ≥3 independent experiments, each symbol representing (**b,d**) independent experiments in which cells from 3-5 mice were pooled by group (b,d: n=3,6, respectively) or (**f**) independent co-culture experiments (BMDCs; BMDCs+AF647-HDM; BMDCs+PBS neutr.+AF647-HDM; BMDCs+LPS^{lo} neutr.+AF647-HDM; BMDCs+LPS^{lo} neutr.+AF647-HDM+DNAse; BMDCs+ LPS^{hi} neutr.+AF647-HDM: n=6;9;4;9;6;4, respectively). *P* values were calculated using (**b**) a two-way or (**d,f**) a one-way ANOVA with Tukey's *post hoc* test. *P<0.05; **P<0.01; ***P<0.001. BMDCs, bone marrow-derived dendritic cells; MFI, mean fluorescence intensity; ns, not significant.
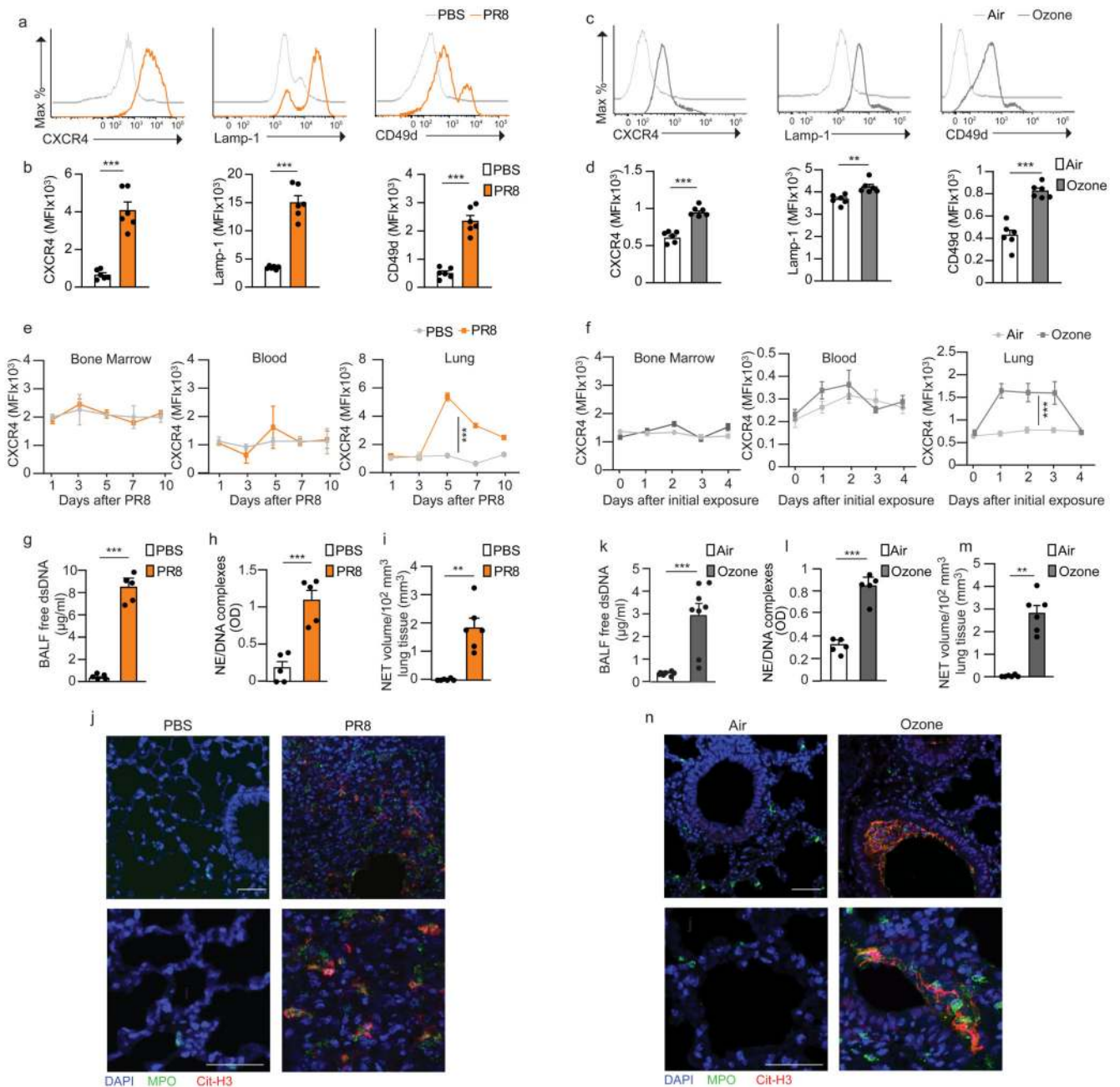
Figure 7. Influenza virus infection and ozone exposure instruct recruited lung CXCR4^{hi} neutrophils to release NETs.

a,**c**, Representative histograms of CXCR4, Lamp-1 and CD49d expression by lung CD45$^+$CD11b$^+$Ly-6G$^+$ neutrophils (**a**) 7 days after influenza virus (PR8) infection or (**c**) 24 h after 3 daily ozone exposures. **b,d**, MFI showing quantification of CXCR4, CD49d and Lamp-1 expression by lung CD45$^+$CD11b$^+$Ly-6G$^+$ neutrophils as in a and c, respectively. **e,f**, Kinetic analysis of CXCR4 expression by bone marrow, blood and lung CD45$^+$CD11b$^+$Ly-6G$^+$ neutrophils after (**e**) PR8 infection or (**f**) ozone exposure, as in a. **g,k**, Levels of extracellular dsDNA in the BALF of (**g**) PBS-injected and PR8-infected mice, 7 days after

PR8, or (**k**) air- and ozone-exposed mice, 24 h after 3 daily ozone exposures. **h,l**, ELISA measurement of NE/DNA complexes in the BALF of mice as in g and k, respectively. **i,m**, Confocal microscopy stainings of Cit-H3⁺MPO⁺ NETs on lung sections of mice as in g and k, respectively. Pictures are representative of one of >5 lungs analyzed. **j,n**, Quantification of NET volume in lung sections of mice as in g and k, respectively. (**b,d-i,k-m**) Data show mean + s.e.m. and are pooled from (**b,d,g-i,k-m**) 2-3 independent experiments (b,d,g,h,i,k,l,m: n=6,6,5,5,6,8,5,6) mice/group, respectively), or (**e,f**) 2 independent experiments per time point analyzed (n=4 mice/time point). P values were calculated using (**b,d,g-i,k-m**) an unpaired two-tailed Student's t test or (**e,f**) a one-way ANOVA that compares PR8-infected or ozone-exposed vs. control counterparts. **P<0.01; ***P<0.001. BALF, bronchoalveolar lavage fluid; ns, not significant; OD, optical density. Scale bars = 50 µm.
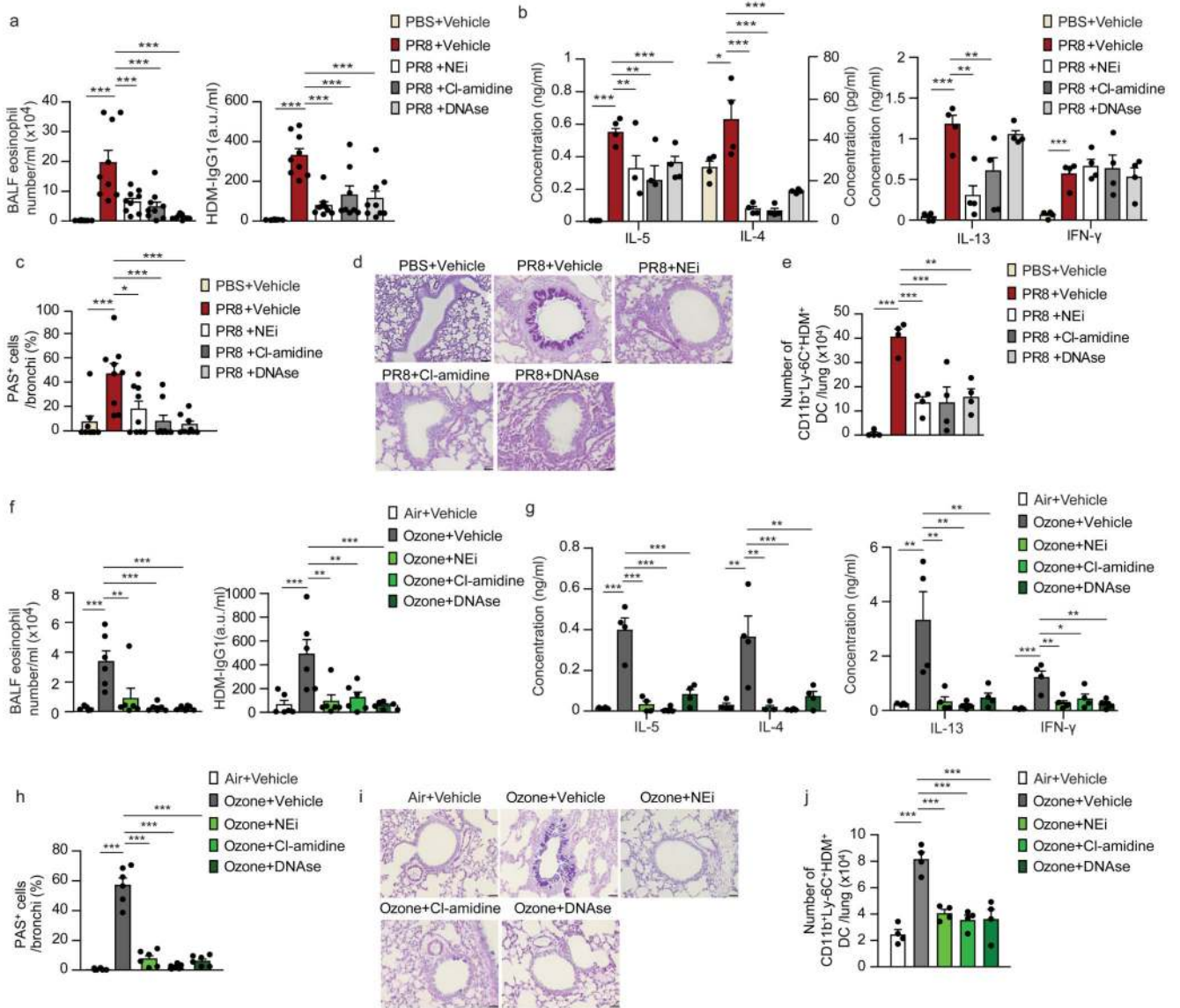
Figure 8. NETs mediate influenza virus- and ozone-potentiated type 2 allergic airway inflammation to HDM.

a, Eosinophil cell counts in the BALF (left) and ELISA measurement of HDM-specific IgG1 in the serum (right), assessed 3 days after the second HDM administration in vehicle-HDM and PR8-HDM mice treated daily for 12 days with DNAse i.p., starting 5 days after PR8, or treated every 12 h with NEi or Cl-amidine i.p., for the same duration as for DNAse. **b**, ELISA measurement of cytokine production by HDM-restimulated BLN cells of mice as in a. **c**, Quantification of PAS-stained epithelial cells per bronchi showing airway mucus production in mice as in a. **d**, Representative PAS staining of lung sections of mice as in a. **e**, Absolute numbers of lung CD11b^{+}Ly-6C^{+}AF647-HDM^{+} DCs assessed 8 days after PR8 and 24 h after AF647-HDM in vehicle-AF647-HDM and PR8-AF647-HDM mice treated daily for 3 days with DNAse i.p., starting 5 days after PR8, or treated every 12 h with NEi or Cl-amidine i.p., for the same duration as for DNAse. **f**, Eosinophil cell counts in the BALF

(left) and ELISA measurement of HDM-specific IgG1 in the serum (right), assessed 3 days after the second HDM administration in vehicle-HDM and ozone-HDM mice treated daily for 4 days with DNAse i.p., starting the first day of ozone exposure, or treated every 12 h with NEi or Cl-amidine i.p., for the same duration as for DNAse. **g**, ELISA measurement of cytokine production by HDM-restimulated BLN cells of mice as in f. **h**, Quantification of PAS-stained epithelial cells per bronchi showing airway mucus production in mice as in f. **i**, Representative PAS staining of lung sections of mice as in f. **j**, Absolute numbers of lung CD11b$^+$Ly-6C$^+$AF647-HDM$^+$ DCs assessed 2 days after the last ozone exposure and 24 h after AF647-HDM in mice as in f. (**a-c,e,f-h,j**) Data show mean + s.e.m. and are pooled from 2-3 independent experiments, each symbol representing (**a,c,f,h**) individual mice (a,b,e,g,h,k: n=9,9,6,6 mice/group, respectively) or (**b,e,g,j**) independent experiments in which cells from 2-4 mice were pooled by group. *P* values were calculated using a one-way ANOVA with Tukey's *post hoc* test. *P<0.05; **P<0.01; ***P<0.001. BALF, bronchoalveolar lavage fluid; a.u., arbitrary unit; ns, not significant. Scale bar = 32 μm.